SIGNAL ANALYSIS USING WAVELET TRANSFORM

by

LIEUTENANT RANEN ADHIKARY

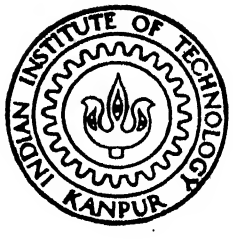

DEPARTMENT OF ELECTRICAL ENGINEERING

INDIAN INSTITUTE OF TECHNOLOGY KANPUR

FEBRUARY, 1992

SIGNAL ANALYSIS USING WAVELET TRANSFORM

A Thesis Submitted
In Partial Fulfilment of the Requirements
for the Degree of
MASTER OF TECHNOLOGY

by
LIEUTENANT RANEN ADHIKARY

to the
DEPARTMENT OF ELECTRICAL ENGINEERING
INDIAN INSTITUTE OF TECHNOLOGY KANPUR
FEBRUARY, 1992

EE-1992-M-ADH-SIG

CERTIFICATE

This is to certify that the thesis work entitled **"SIGNAL ANALYSIS USING WAVELET TRANSFORM"** has been carried out by Lt. Ranen Adhikary under my supervision and has not been submitted elsewhere for a degree.

S Gupta

Dr. (Mrs.) Sumana Gupta
Assistant Professor
Department of Electrical Engineering
Indian Institute of Technology
KANPUR

To

the Almighty

ABSTRACT

The thesis is about signal analysis using wavelet transform. Wavelet theory, which has gained a lot of momentum has been investigated. Various orthogonal basis function which make up the wavelets have been analysed. The corresponding wavelets have been found out. The filters based on the wavelets/orthogonal basis functions have been designed. A computer program has been developed to do the decomposition and reconstruction of signals based on an iterative algorithm. The signals which have been taken up for analysis are composite exponentials and sinusoidal. The same signals with closely spaced bursts and noise have also been taken up for investigation. A signals have also been decomposed and reconstructed by using another scheme called Laplacian Pyramid Scheme.

A separation of exponentials, an age old problem, has also been taken up for investigation in this context. The purpose of this investigation is to see whether by during wavelet decomposition and reconstruction, the exponentials which constitute the original signal, surface or not

ACKNOWLEDGEMENTS

I would like to express my sincere gratitude to Dr.(Mrs) Sumana Gupta for her counsel and guidance. She has been a constant source of inspiration and motivation during the entire thesis work.

Also I am grateful to Dr. P. Gupta Bhaya for his suggestions.

RANEN ADHIKARY

TABLE OF CONTENTS

		PAGE
LIST OF TABLES		vii
LIST OF FIGURES		viii
CHAPTER 1 :	**INTRODUCTION**	1
CHAPTER 2 :	**WAVELET THEORY**	
2.1	Notation	5
2.2	Multiresolution Transform	6
2.3	The Wavelet Representation	15
2.4	Multiresolution Pyramid	24
2.5	Subband Coding Scheme	27
2.6	Laplacian Pyramidal Multiresolution Decomposition and Reconstruction	28
2.7	Comparison between Short-time Fourier Transform and Wavelet Transform	33
CHAPTER 3 :	**RESULTS**	
3.1	Design of Wavelet	43
3.2	Design of Filters	46
3.3	Transfer Function of Filters	48
3.4	Decomposition and Reconstruction by Wavelet Transform	48
3.5	Decomposition and Reconstruction by Laplacian Pyramid Scheme	60
3.6	Energy Plots of Detail Signals	66
3.7	Separation of Exponentials	66
CHAPTER 4 :	**CONCLUSIONS**	78
LIST OF REFERENCES		80

LIST OF TABLES

TABLE		PAGE
3.1	Impulse response of h (Haar basis)	46
3.2	Impulse response of h (Linear Spline)	47
3.3	Impulse response of h (Quadratic Spline)	47
3.4	Impulse response of h (Cubic Spline)	48

LIST OF FIGURES

FIGURE		PAGE
2.1	Algorithm for Decomposition of a Signal	21
2.2	Algorithm for Reconstruction of a Signal	23
2.3	Pyramid Scheme	26
2.4	Subband Coding Scheme	29
2.5	Laplacian Pyramid Scheme	32
2.6	Phase-Space STFT	35
2.7	Phase-Space - Wavelet Transform	42
3.1	Transfer Function of g (Linear Spline)	49
3.2	Transfer Function of h (Linear Spline)	50
3.3	Reconstruction of Exponential (Cubic Spline)	52
3.4	Reconstruction of Exponential (Linear Spline)	53
3.5	Reconstruction of Sinusoid (Cubic Spline)	54
3.6	Reconstruction of Sinusoid (Linear Spline)	55
3.7	Reconstruction of Exponential with Noise (Cubic Spline)	57
3.6	Reconstruction of Exponential with Noise (Linear Spline)	58
3.7	Reconstruction of Sinusoid with Noise (Cubic Spline)	59
3.8	Exponential with Spikes	61
3.9	Reconstruction of Exponential with Spikes (Cubic Spline)	62
3.10	Reconstruction of Exponential with Spikes (Linear Spline)	63
3.11	Sinusoid with Spikes	64
3.12	Reconstruction of Exponental with Pyramid Scheme	65

FIGURE		PAGE
3.13	Reconstruction of Sinusoid with Pyramid Scheme	67
3.14	Energy of Detail Signal of Sinusoid with Spikes at resolution 0.5	68
3.15	Energy of Detail Signal of Sinusoid with Spikes at resolution 0.25	69
3.16	Energy of Detail Signal of Sinusoid with Spikes at resolution 0.125	70
3.17	Energy of Detail Signal of Sinusoid with Spikes at resolution 0.0625	71
3.18	Reconstruction of Exponential (Time constant varying) Linear Spline	73
3.19	Exponential Signals (Time constant varying)	74
3.20	Exponential Signals (Amplitude varying)	75
3.21	Reconstruction of Exponential (Amplitude varying) Linear Spline	76

CHAPTER - 1

INTRODUCTION

Wavelet theory, which has of late has generated a lot of interest, provides a unified framework for a number of techniques which had been developed independently for various signal processing applications. Multiresolution signal processing used in computer vision, sub-band coding of speech and image compression and wavelet series expansions developed in applied mathematics, are all different views of single theory.

The wavelet theory, which covers quite a large area, treats both the continuous and discrete-time cases. It provides very general techniques that can be applied to many tasks in signal processing and hence, has numerous potential applications. In particular, the Wavelet Transform (WT) is of interest for the analysis of non-stationary signals, because it provides an alternative to the classical Short-Time Fourier Transform (STFT) or Gabor transform. The basic difference between WT and STFT is that in contrast to the STFT, which uses a ~~single~~ ~~uses~~ a single analysis window, the WT uses short windows at high frequencies and long windows at low frequencies.

The Wavelet Transform can be seen as a signal decomposition onto a set of basis functions. In fact, basis functions called wavelets always underlie the wavelet analysis. They are obtained from a single prototype wavelet by dilations and contractions

(scalings) as well as shifts. The prototype wavelet can be thought of as a bandpass filter.

In a Wavelet Transform, the notion of scale is introduced as an alternative to frequency, leading to a so-called time-scale representation. In other words, a signal is mapped into a time-scale plane in contrast to the time-frequency plane used in STFT.

There are several types of wavelet transforms. The choice of a transform depends on the type of application. For example, for a continuous input signal, the time and scale parameters can be continuous, leading to the continuous wavelet transform. They may be discrete also, giving rise to a Wavelet Series Expansion. Or the wavelet transform can be defined for discrete-time signals, which is known as Discrete Wavelet Transform (DWT). In the latter case, it uses Multirate Signal Processing techniques. In this context, one can draw an analogy with the Fourier Transform (continuous), Fourier Series and Discrete Fourier Transform.

Wavelet theory has been developed as a unifying framework only recently, although similar ideas and constructions took place as early as the beginning of the century. The idea of looking at a signal at various scales and analysing it with various resolutions has in fact emerged independently in many different fields. In mid-eighties, researchers such as Morlet, Grossmann, and Meyer built strong mathematical foundations around the subject.

The attention of the signal processing community was soon caught when Daubechies and Mallats, in addition to their contribution to the theory of wavelets, established connections to the discrete signal processing results.

In the paper presented, various bases of wavelets have been investigated. The frequency response of the filters corresponding to the bases have been explored. In addition, a comparison between Wavelet Transform and Short-Time Fourier Transform has been drawn. A study has been carried out on the decomposition and reconstruction of composite signals such as exponentials with varied time constants and sinusoidals with varied frequencies, with the help of the wavelet transform and Laplacian Pyramid Scheme. The reconstruction of the above mentioned signals with bursts and noise have also been examined. The separation of exponentials, a problem which researchers have been trying to solve using various methods, is of great significance and importance in some fields such as physics. The problem has been looked into from the Wavelet Transform point of view.

In the thesis, Chapter 2 deals with the multiresolution transform and its implementation, the wavelet representation, pyramidal algorithm, comparison between wavelet trasnform and short time fourier transform, and Laplacian pyramid algorithm.

In Chapter 3, we have described the results of various designs and operations. The chapter also deals with the design of wavelets and filters corresponding to different orthogonal basis

functions. The results of reconstruction of exponential and sinusoidal signals have been described. In this chapter, we also discuss the problem of separation of exponentials with regards to wavelet transform.

Conclusion has been drawn in Chapter 4.

CHAPTER - 2

WAVELET THEORY

2.1 NOTATION

a) Z & R denote the set of integers and real numbers respectively. $L^2(R)$ denotes the vector space of measurable, square integrable one-dimensional functions f(x).

b) For $f(x) \in L^2(R)$ and $g(x) \in L^2(R)$, the inner product of f(x) with g(x) is given by

$$\langle g(u), f(u) \rangle = \int_{-\infty}^{\infty} g(u).f(u)\, du$$

c) The norm of f(x) is $L^2(R)$ is given by

$$\| f \|^2 = \int_{-\infty}^{\infty} |f(u)|^2\, du$$

d) The convolution of two functions $f(x) \in L^2(R)$ and $g(x) \in L^2(R)$ is denoted by

$$f * g(x) = \left[f(u) * g(u) \right] (x)$$

$$= \int_{-\infty}^{\infty} f(u).g(x-u)\, du$$

e) The Fourier Transform of $f(x) \in L^2(R)$ is written $\hat{f}(w)$ and is defined by

$$\hat{f}(w) = \int_{-\infty}^{\infty} f(x) \exp(-wx)\, dx$$

(f) $I^2(Z)$ is the vector space of square summable sequences

$$I^2(Z) = \left\{ \left(\alpha_i\right)_{i\in Z} \quad \sum_{i=-\infty}^{\infty} |\alpha_i|^2 < \infty \right\}$$

2.2 MULTIRESOLUTION TRANSFORM

2.2.1 Multiresolution Approximation of $L^2(R)$ [2]

Let A_2j be the operator which approximates a signal at resolution 2^j. We suppose that our original signal $f(x)$ is measurable and has a finite energy : $f(x) \in L^2(R)$. Here, we characterize A_2j from the intuitive properties that one would expect from such an approximation operator. We state each property in words, and then give the equivalent mathematical formulation.

(i) A_2j is a linear operator. If $A_2jf(x)$ is the approximation of some function $f(x)$ at the resolution 2^j; then $A_2jf(x)$ is not modified if we approximate it again at the resolution 2^j. This principle shows that A_2j is a projection operator on a particular vector space $V_2j \subset L^2(R)$. The vector space V_2j can be interpreted as the set of all possible approximations at the resolution 2^j of functions in $L^2(R)$.

(ii) Among all the approximated functions at the resolution 2^j, $A_2jf(x)$ is the function which is the most similar to $f(x)$.

$$\forall\, g(x) \in V_2j,\ \|g(x)-f(x)\| \geq \|A_2jf(x) - f(x)\| \qquad (2.1)$$

Hence, the operator $A_2 j$ is an orthogonal projection on the vector space $V_2 j$.

(iii) The approximation of a signal at a resolution 2^{j+1} contains all the necessary information to compute the same signal at a smaller resolution 2^j. This is a causality property. Since $A_2 j$ is a projection operator on $V_2 j$, this principle is equivalent to

$$\forall j \in Z, \quad V_2 j \subset V_2 j+1 \tag{2.2}$$

(iv) An approximation operation is similar at all resolutions. The spaces of approximated functions should thus be derived from one another by scaling each approximated function by the ratio of their resolution values.

$$\forall j \in Z, \quad f(x) \in V_2 j \iff f(2x) \in V_2 j+1 \tag{2.3}$$

(v) The approximation $A_2 jf(x)$ of a signal $f(x)$ can be characterized by 2^j samples per length unit. When $f(x)$ is translated by a length proportional to 2^{-j}, $A_2 jf(x)$ is translated by the same amount and is characterized by the same samples which have been translated. As a consequence of (2.3), it is sufficient to express the principle (V) for the resolution j=o. The mathematical translations consist of the following

. **Discrete characterization :**

There exists an isomorphism I from V_1 onto $l^2(Z)$ (2.4)

. Translation of the approximation :

$$\forall k \in Z, \quad A_1 f_k(x) = A_1 f(x-k). \quad \text{where } f_k(x) = f(x-k) \qquad (2.5)$$

. Translation of the samples :

$$I\left[A_1 f(x)\right] = \left[\alpha_i\right]_{i \in Z} \iff I\left[A_1 f_k(x)\right] = \left[\alpha_{i-k}\right]_{i \in Z} \qquad (2.6)$$

(vi) When computing an approximation of f(x) at resolution 2^j, some information about f(x) is lost. However, as the resolution increase to $+\infty$, the approximated signal should converge to the original signal. Conversely as the resolution decreases to zero, the approximated signal contains less and less information and converges to zero.

Since the approximated signal at a resolution 2^j is equal to the orthogonal projection on a space $V_2 j$, this principle can be written

$$\lim_{j \to +\infty} V_2 j = \overset{+\infty}{\underset{j=-\infty}{\cup}} V_2 j \quad \text{is dense in } L^2(R) \qquad (2.7)$$

and

$$\lim_{j \to -\infty} V_2 j = \overset{+\infty}{\underset{j=-\infty}{\cap}} V_2 j = \left\{ 0 \right\} \qquad (2.8)$$

We call any set of vector spaces $\left[V_2 j\right]_{j \in Z}$ which satisfies the properties (2.2)-(2.8) a multiresolution approximation of $L^2(R)$. The associated set of operators $A_2 j$ satisfying (i) and (vi) give the approximation of any $L^2(R)$ function at a resolution 2^j. We now give a simple example of a multiresolution approximation of $L^2(R)$.

Example : Let V_1 be the vector space of all functions of $L^2(R)$ which are constant on each interval $]K,K+1[$ for any $k \in Z$. Equation (2.3) implies that $V_2 j$ is the vector space of all the functions of $L^2(R)$ which are constant on each interval $]k2^{-j}, (k+1)2^{-j}[$, for any $k \in Z$. The condition (2.2) is easily verified. We can define an isophormism I which satisfies properties (2.4), (2.5) and (2.6) by association with any function $f(x) \in V_1$ the sequence $(\alpha_k)_{k \in Z}$ such that α_k equals the value of $f(x)$ on the interval $]k, k+1[$. We know that vector space of piecewise constant functions is dense in $L^2(R)$. Hence we can derive that $\bigcup_{j=-\infty}^{\infty} V_2 j$ is dense in $L^2(R)$. It is clear that $\bigcap_{j=-\infty}^{\infty} V_2 j = \{0\}$, so the sequence of vector spaces $\left(V_2 j\right)_{j \in Z}$ is a multiresolution approximation of $L^2(R)$. Unfortunately, the functions of these vector spaces are neither smooth nor continuous, making this multiresolution approximation rather inconvenient.

We saw that the approximation operator $A_2 j$ is an orthogonal projection on the vector space $V_2 j$. In order to numerically characterize this operator, we must find an orthogonal basis of $V_2 j$. The following theorem shows that such an orthogonal basis can be defined by dilating and translating a unique function $\phi(x)$.

Theorem 1 : Let $\left(V_2 j\right)_{j \in Z}$ be a multiresolution approximation of $L^2(R)$. There exists a unique function $\phi(x) \in L^2(R)$, called the scaling function, such that if we set $\phi_2 j(x) = 2^j \phi(2^j x)$ for $j \in Z$, (the dialation of $\phi(x)$ by 2^j), then

$$\left(\sqrt{2^{-j}}\phi_2 j\left[x-2^{-j}n\right]\right)_{n\in Z} \text{ is an orthogonal basis of } V_2 j. \qquad (2.9)$$

The theorem shows that we can build an orthonormal basis of any $V_2 j$ by dilating a function $\phi(x)$ with a coefficient 2^j and translating the resulting function with a grid whose interval is proportional to 2^{-j}. The function $\phi_2 j(x)$ are normalized with respect to $L^1(R)$ norm. The coefficient $\sqrt{2^{-j}}$ appears in the basis set in order to normalize the functions in the $L^2(R)$ norm. For a given multiresolution approximation $(V_2 j)_{j\in Z}$, there exists a unique scaling function $\phi(x)$, which satisfies (2.9). However, for different multiresolution approximations, the scaling functions are different.

The orthogonal projection on $V_2 j$ can now be computed by decomposing the signal f(x) on the orthogonal basis given by Theorem 1. Specifically,

$$\forall\ f(x) \in L^2(R),$$

$$A_2 jf(x) = 2^{-j} \sum_{n=-\infty}^{\infty} < f(u),\ \phi_2 j\ (u-2^{-j}n) > \phi_2 j\ (x-2^{-j}n) \qquad (2.10)$$

The approximation of the signal f(x) at the resolution 2^j, $A_2 jf(x)$, is thus characterized by the set of inner products which we denote by

$$A_2^d j\ f = \left(< f(u),\ \phi_2 j(u-2^{-j}n) >\right)_{n\in Z} \qquad (2.11)$$

$A_2^d jf$ is called a discrete approximation of f(x) at the resolution 2^j. Each inner product can also be interpreted as a convolution product evaluated at a point $2^{-j}n$

$$\langle f(u), \phi_2 j(u-2^{-j}n) \rangle = \int_{-\infty}^{\infty} f(u).\phi_2 j(u-2^{-j}n)\, du$$

$$= (f(u) * \phi_2 j(-u))\ (2^{-j}n)$$

Hence, we can rewrite $A_2^d jf$:

$$A_2^d jf = \left[(f(u) * \phi_2 j(-u)\right]\ \left[2^{-j}n)\right]_{n\in Z} \qquad (2.12)$$

Since $\phi(x)$ is a lowpass filter, this discrete signal can be interpreted as a lowpass filtering of f(x) followed by a uniform sampling at the rate 2^j. In an approximation operation, when removing the details of f(x) smaller than 2^{-j}, we suppress the highest frequencies of this function. The scaling function $\phi(x)$ forms a very particular lowpass filter since the family of functions $\left[\sqrt{2^{-j}}\ \phi_2 j(x-2^{-j}n)\right]_{n\in Z}$ is an orthonormal family.

2.2.2 Implementation of a Multiresolution Transform [2]

In practice, a physical measuring device can only measure signal at a finite resolution. For normalization purposes, we suppose that this resolution is equal to 1. Let $A_1^d f$ be the discrete approximation at the resolution 1 that is measured. The causality principle says that from $A_1^d f$ we can compute all the discrete approximations $A_2^d j$ for $j<0$. In this

section, a simple iterative algorithm is described for calculating these discrete approximations.

Let $(V_2 j)_{j \in Z}$ be a multiresolution approximation and $\phi(x)$ be the corresponding scaling function. The family of functions $(\sqrt{2^{-j-1}}\phi_2 j+1(x-2^{-j-1}k))_{k \in Z}$ is an orthonormal basis of $V_2 j+1$. We know that for any $n \in Z$, the function $\phi_2 j(x-2^{-j}n)$ is a member of $V_2 j$ which is included in $V_2 j+1$. It can thus be expanded in this orthonormal basis of $V_2 j+1$:

$$\phi_2 j(x-2^{-j}n) =$$

$$2^{-j-1} \sum_{K=-\infty}^{\infty} < \phi_2 j(u-2^{-j}n) \phi_2 j+1(u-2^{-j-1}k) > \phi_2 j+1(x-2^{-j-1}k) \qquad (2.13)$$

By changing variables in the inner product integral, one can show that

$$2^{-j-1} < \phi_2 j(u-2^{-j}n), \phi_2 j+1(u-2^{-j-1}k) >$$
$$= < \phi_2 -1(u), \phi(u-(k-2n)) >$$

When computing the inner products of $f(x)$ with both sides of (2.13), we obtain

$$< f(u), \phi_2 j(u-2^{-j}n) > = \sum_{k=-\infty}^{\infty} < \phi_2 -1(u), \phi(u-(k-2n)) >$$
$$< f(u), \phi_2 j+1(u-2^{-j-1}k) > \qquad (2.14)$$

Let H be the discrete filter whose impulse response is given by

$$\forall n \in Z \ . \ h(n) = \langle \phi_2{}^{-1}(n), \phi(u-n) \rangle \qquad (2.15)$$

Let $\tilde{H}$ be the mirror filter with impulse response $\tilde{h}(n) = h(-n)$. By inserting (2.15) in the previous equation, we have

$$\langle f(u), \phi_2{}^j (u-2^{-j}n) \rangle = \sum_{k=-\infty}^{\infty} \tilde{h}\ (2n-k) \langle f(u), \phi_2{}^{j+1}(u-2^{-j-1}k) \qquad (2.16)$$

Equation (2.16) shows that $A_2^d jf$ can be computed by the convolution of $A_2^d j+1f$ and $\tilde{H}$ and keeping every other sample of the output. All the discrete approximations $A_2^d jf$, for $j < 0$; can thus be computed from $A_1^d f$ by repeating this process. This operation is called a pyramid transform. The algorithm is illustrated by a block diagram later in the chapter (Fig. 2.1).

In practice, the measuring device gives only a finite number of samples : $A_1^d f = (\alpha_n)_{1 \le n \le N}$. Each discrete signal $A_2^d jf (j<0)$ has $2^j N$ samples. In order to avoid border problems, when computing the discrete approximations $A_2^d jf$, we suppose that the original signal $A_1^d f$ is symmetric with respect to n=0 and n=N.

$$\alpha_n = \begin{cases} \alpha_{-n} & \text{if } -N < n < 0 \\ \alpha_{2N-n} & \text{if } 0 < n < N \end{cases}$$

If the impulse response of the filter $\tilde{H}$ is even ($\tilde{H}$=H), each discrete approximation $A_2^d jf$ will also be symmetric with respect to n=0 and $n=2^{-j}N$.

Theorem 1 shows that a multiresolution approximation $(V_2 j)_{j \in Z}$ is completely characterized by the scaling function, $\phi(x)$. A scaling function can be defined as a function $\phi(x) \in L^2(R)$ such that, for all $j \in Z$, $\left[\sqrt{2^{-j}}\ \phi_2 j(x-2^{-j}n)\right]_{n \in Z}$ is an orthonormal family, and if $V_2 j$ is the vector space generated by this family of functions, then $(V_2 j)_{j \in Z}$ is a multiresolution approximation of $L^2(R)$.

Theorem 2 : Let $\phi(x)$ be a scaling function and let H be a discrete filter with impulse response $h(n) = \langle \phi_2 -1(u),\ \phi(u-n) \rangle$. Let H(w) be the Fourier Transform defined by

$$H(\omega) = \sum_{n=-\infty}^{\infty} h(n)\ e^{-jn\omega} \qquad (2.17)$$

H(w) satisfies the following two properties :

$$H(0) = 1 \qquad (2.17a)$$

and

$$|H(\omega)|^2 + |H(\omega + \pi)|^2 \qquad (2.17b)$$

Conversely, $|H(\omega)| \neq 0 \quad$ for $\quad \omega \in [0,\ \pi/2]$ (2.17c)

The function defined by

$$\hat{\phi}\ (\omega) = \prod_{p=1}^{+\infty} H(2^{-P}\omega) \qquad (2.18)$$

is the Fourier transform of a scaling function.

The filters that satisfy property (2.17b) are called conjugate filters. Given a conjugate filter H which satisfies

(2.17a) - (2.17c), we can then compute the Fourier transform of the corresponding scaling function with (2.16). One can easily show that the corresponding function $H(\omega)$ satisfies

$$H(\omega) = \exp(-j\omega)\cos(\omega/2)$$

2.3 THE WAVELET REPRESENTATION

In this section, multiresolution representation based on the differences of the information available at two successive resolutions 2^j and 2^{j+1} is developed. It is shown that such a representation can be computed by decomposing the signal using a wavelet orthonormal basis.

2.3.1 The Detail Signal [2]

Here, we explain how to extract the difference of information called the detail signal at the resolution 2^j. The approximation at the resolution 2^{j+1} and 2^j of a signal are respectively equal to its orthogonal projection on $V_2 j+1$ and $V_2 j$. By applying the projection theorem, it can be easily shown that the detail signal at the resolution 2^j is given by the orthogonal projection of the original signal on the orthogonal complement of $V_2 j$ in $V_2 j+1$. Let $O_2 j$ be this orthogonal complement i.e.

$O_2 j$ is orthogonal to $V_2 j$,

$O_2 j \oplus V_2 j = V_2 j+1$.

To compute the orthogonal projection of a function $f(x)$ on $O_2 j$, it is required to find an orthonormal basis of $O_2 j$.

Theorem 3 shows that such a basis can be built by scaling and translating a function $\psi(x)$.

Theorem 3 : Let $(V_2 j)_{j \in Z}$ be a multiresolution vector space sequence, $\phi(x)$ the scaling function, and H the corresponding conjugate filter. Let $\psi(x)$ be a function whose Fourier transform is given by

$$\hat{\psi}(\omega) = G(\omega/2).\hat{\phi}(\omega/2)$$

$$\text{with} \quad G(\omega) = e^{j\omega}\,\overline{H(\omega+\pi)} \tag{2.19}$$

Let $\psi_2 j(x) = 2^j \psi(2^j x)$ denote the dilation of $\psi(x)$ by 2^j. Then $(\sqrt{2^{-j}}\ \psi_2 j(x-2^{-j}n))_{n \in Z}$ is an orthonormal basis of $O_2 j$ and $(\sqrt{2^{-j}}\ \psi_2 j(x-2^{-j}n))_{(n,\, j) \in Z}$ is an orthonomal basis of $L^2(R)$. $\psi(x)$ is called an orthonomal wavelet. An orthonormal basis of $O_2 j$ can thus be computed by scaling the wavelet $\psi(x)$ with a coefficient 2^j and translating it on a grid whose interval is proportional to 2^{-j}.

The decomposition of a signal in an orthonormal wavelet basis gives an intermediate representation between Fourier and spatial representations. Due to this double localization in the Fourier and Spatial domains, it is possible to characterize the local regularity of a function f(x) based on the coefficients in a wavelet orthonormal basis expansion.

Let $P_{O_2 j}$ be the orthonormal projection on the vector space $O_2 j$. As a consequence of Theorem 3, this operator can now be written

$$P_{O_2 j} f(x) = 2^{-j} \sum_{n=-\infty}^{\infty} \langle f(u), \psi_2 j(u-2^{-j}n) \rangle . \psi_2 j(x-2^{-j}n) \quad (2.20)$$

$P_{O_2 j} f(x)$ yields to the detail signal of $f(x)$ at the resolution 2^j. It is characterized by the set of inner products

$$D_2 jf = \left[\langle f(u), \psi_2 j(u-2^{-j}n) \rangle \right]_{n \in Z} \quad (2.21)$$

$D_2 jf$ is called the Discrete Detail Signal at the resolution 2^j. It contains the difference of information between $A_2^d j+1 f$ and $A_2^d jf$. It can be shown that each of these inner products is equal to the convolution of $f(x)$ with $\psi_2 j(-x)$ evaluated at $2^{-j}n$

$$\langle f(u), \psi_2 j(u-2^{-j}n) \rangle = \left[f(u) * \psi_2 j(-u) \right] \left[2^{-j}n \right] \quad (2.22)$$

Equations (2.21) and (2.22) show that the discrete detail signal at the resolution 2^j is equal to a uniform sampling of $(f(u) * \psi_2 j(-u)(x))$ at the rate 2^j,

$$D_2 jf = \left[(f(u) * \psi_2 j(-u) \ (2^{-j}n) \right]_{n \in Z}$$

The wavelet $\psi(x)$ can be viewed as a bandpass filter whose frequency bands are approximately equal to $[-2\pi, -\pi] \cup [\pi, 2\pi]$. Hence, the detail signal $D_2 jf$ describes $f(x)$ in the frequency bands $\left[-2^{-j+1}\pi, -2^{-j}\pi \right] \cup \left[2^{-j}\pi, 2^{-j+1}\pi \right]$.

It can be proved that by induction that for any $J > 0$, the original discrete signal $A_1^d f$ measured at the resolution 1 is represented by

$$\left[A_2^d - jf, (D_2 jf)_{-J \le j \le -1} \right] \quad (2.23)$$

This set of discrete signals is called an orthogonal wavelet representation, and consists of the reference signal at a coarse resolution $A_2^d - jf$ and the detail signals at the resolutions 2^j for $-J \leq j \leq -1$. It can be interpreted as a decomposition of the original signal in an wavelet basis.

2.3.2 Implementation of an Orthogonal Wavelet Representation [2]

In this section, we describe a pyramidal algorithm to compute the wavelet representation.

For any $n \in Z$, the function $\psi_2 j(x-2^{-j}n)$ is a member of $O_2 j \subset V_2 j+1$. In the same manner as (2.13), this function can be expanded in an orthonormal basis of $V_2 j+1$.

$$\psi_2 j(x-2^{-j}n) = 2^{-j-1} \sum_{k=-\infty}^{\infty} < \psi_2 j\ (u-2^{-j}n),\ \phi_2 j+1\ (u-2^{-j-1}k) > \cdot\ \phi_2 j+1\ (x-2^{-j-1}k) \qquad (2.24)$$

As we did in (2.14), by changing the variables in the inner integral we can prove that

$$2^{-j-1} < \psi_2 j(u-2^{-j}n),\ \phi_2 j+1(u-2^{-j-1}k) >$$

$$= < \psi_2 -1(u),\ \phi(u-(k-2n)) > \qquad (2.25)$$

Hence, by computing the inner product of f(x) with the functions of both sides of (2.24), we obtain

$$< f(u),\ \psi_2 j(u-2^{-j}n) > =$$

$$\sum_{k=-\infty}^{\infty} < \psi_2 -1(u),\ \phi(u-(k-2n)) > .<f(u),\phi_2 j+1(u-2^{-j-1}k)> \quad (2.26)$$

Let G be the discrete filter with impulse response.

$$g(n) = < \psi_2 -1(u),\ \phi(u-n) > \quad (2.27)$$

$\tilde{G}$ be the mirror filter with impulse response $\tilde{g}(n) = g(-n)$. Inserting (2.27) to (2.26) yields

$$< f(u),\ \psi_2 j(u-2^{-j}n) > = D_2 jf$$

$$= \sum_{k=-\infty}^{\infty} \tilde{g}\ (2n-k) <f(u),\ \phi_2 j+1\ (u-2^{-j-1}k)> \quad (2.28)$$

Equation (2.28) shows that we can compute the detail signal $D_2 jf$ by convolving $A_2^d j+1f$ with the filter $\tilde{G}$ and retaining every other sample of the output. The orthogonal wavelet representation of a discrete signal $A_1^d f$ can therefore be computed by successively decomposing $A_2^d j+1f$ into $A_2^d jf$ and $D_2 jf$ for $-J \leq j \leq -1$.

Equation (2.19) of Theorem 3 implies that the impulse response of the filter G is related to the impulse response of the filter H by

$$g(n) = (-1)^{1-n}\ h(1-n) \quad (2.29)$$

G is the mirror filter of H, and is a highpass filter. In signal processing, G and H are quadrature mirror filters. Equation (2.28) can be interpreted as a highpass filtering of the discrete signal $A_2^d j+1f$.

If the original signal has N samples, then the discrete signals D_2jf and $A_2^d jf$ have 2^jN samples each. Thus, the wavelet representation $(A_2^d\text{-}jf, (D_2jf) - J \leq j \leq -1)$ has the same total number of samples as the original approximated signal $A_1^d f$. This occurs because the representation is orthogonal. The energy of the samples of D_2jf gives a measure of the irregularity of the signal at the resolution 2^{j+1}. Whenever $A_dj(x)$ and $A_dj+1f(x)$ were significantly different, the signal detail has a high amplitude. In Fig. 2.1, the implementation of wavelet decomposition of is shown.

2.3.3 Signal Reconstruction from an Orthogonal Wavelet Representation

We have seen that the wavelet representation is complete. We now show that the original discrete signal can also be reconstructed with a pyramid transform. Since O_2j is the orthogonal complement of V_2j in V_2j+1, $(\sqrt{2^{-j}}\phi_2j(x-2^{-j}n), \sqrt{2^{-j}}\psi_2j(x-2^{-j}n))_{n\in Z}$ is an orthogonal basis of V_2j+1. For any $n > 0$, the function $\phi_2j+1(x - 2^{-j-1}n)$ can thus be decomposed in this basis

$$\phi_2 j+1\left[x - 2^{-j-1}n\right]$$

$$= 2^{-j}\sum_{k=-\infty}^{\infty} < \phi_2 j\ (u-2^{-j}k),\ \phi_2 j+1(u-2^{-j-1}n) > .\phi_2 j(x-2^{-j}k)$$

$$+ 2^{-j}\sum_{k=-\infty}^{\infty} < \psi_2 j(u-2^{-j}k),\ \phi_2 j+1\ (u-2^{-j-1}n) > .\psi_2 j(x-2^{-j}k) \qquad (2.30)$$

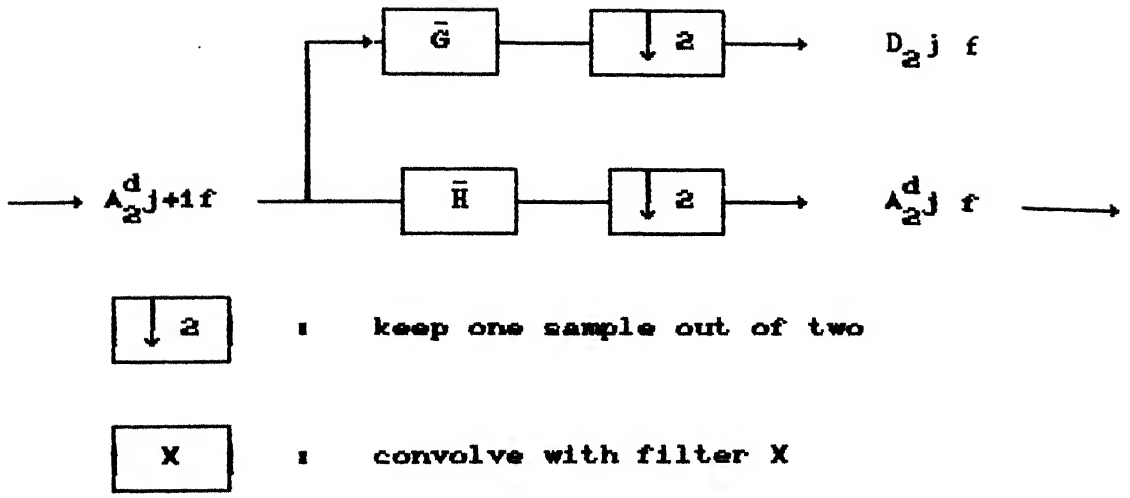

Fig. 21 : Decomposition of a discrete approximation $A_2^d j+1$ into an approximation at a coarser resolution $A_2 j\ f$ and the signal detail $D_2 j\ f$. By repeating in cascade this algorithm for $-1 \geq j \geq -J$; we compute the wavelet representation of a signal $A_2^d j\ f$ on J resolution levels.

By computing the inner product of each side of equation (2.30) with the function f(x) we have

$$< f(u), \phi_2 j+1\ (u-2^{-j-1}) >$$

$$= 2^{-j} \sum_{k=-\infty}^{\infty} < \phi_2 j(u-2^{-j}k), \phi_2 j+1(u-2^{-j-1}n) > \ . \ <f(u),\phi_2 j(u-2^{-j}k)>$$

$$+ 2^{-j} \sum_{k=-\infty}^{\infty} < \psi_2 j\ (u-2^{-j}k), \phi_2 j+1(u-2^{-j-1}n)> <f(u).\psi_2 j(u-2^{-j}k)> \qquad (2.31)$$

Inserting (2.14) and (2.25) in this expression and using the filters H and G, respectively, defined by (2.15) and (2.27) yields

$$<(f(u), \phi_2 j+1\ (u - 2^{-j-1}n)>$$

$$= 2 \sum_{k=-\infty}^{\infty} h(n-2k).<f(u), \phi_2 j\ (u-2^{-j}k)>$$

$$+ 2 \sum_{k=-\infty}^{\infty} g(n-2k) <f(u), \psi_2 j\ (u-2^{-j}k)> \qquad (2.32)$$

This equation shows that $A_2^d j+1$ can be reconstructed by putting zeros between each sample of $A_2^d jf$ and $D_2 jf$ and convolving the resulting signals with the filters H and G, respectively. The block diagram in Fig. 2.2 illustrates this algorithm. The original discrete signal $A_1^d f$ at the resolution 1 is reconstructed

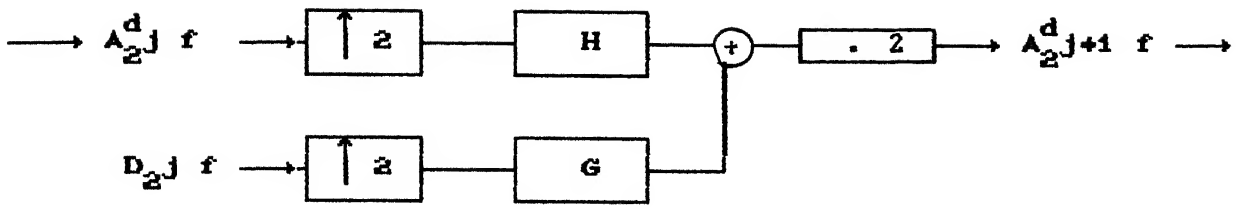

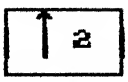

: put one zero between each sample

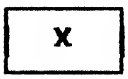

: convolve with filter X

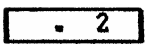

: multiplication by 2

Fig. 2.2 Reconstruction of a discrete approximation $A_2^d j+1\ f$ from an approximation at a coarser resolution $A_2^d j\ f$ and the signal detail $D_2 j\ f$. By repeating in cascade this algorithm for $-J \leq j \leq -1$, we are recostructed from its wavelet representation.

by repeating this procedure for $-J \leq j < 0$. From the discrete approximation $A_1^d f$, we can recover the continuous approximation $A_1 f(x)$ with equation (10).

2.4 MULTIRESOLUTION PYRAMID [4]

Given an original sequence x(n), $n \in Z$, we derive a lower resolution signal by lowpass filtering with a half band lowpass filter having impulse response g(n). Following Nyquist rule, we can subsample by two (drop every other sample), thus describing the scale in the analysis. This results is a signal y(n) given by

$$y(n) = \sum_{k=-\infty}^{\infty} g(k)\, x(2n-k)$$

The resolution change is obtained by the lowpass filter (loss of high frequency detail). The scale change is due to the subsampling by two, since a shift by two in original signal x(n) results in a shift by one in y(n).

Now, based on this lowpass and subsampled version of x(n), we try to find an approximation, a(n), to the original. This is done by first upsampling y(n) by two (that is, inserting a zero between every sample) since we need a signal at the original scale for comparison.

$$y'(2n) = y(n) \quad , \quad y'(2n+1) = 0$$

Then, y'(n) is interpolated with a filter with impulse response g'(n) to obtain the approximation a(n)

$$a(n) = \sum_{k=-\infty}^{\infty} g'(k)\, y'(n-k) \qquad (2.33)$$

Note that if g(n) and g'(n) were perfect halfband filters (having a frequency passband equal to 1 over the normalized frequency range $-\pi/2$ to $\pi/2$ and equal to 0 elsewhere), then the Fourier transform of a(n) would be equal to the Fourier transform of x(n) over the frequency range $(-\pi/2, \pi/2)$ while being equal to zero elsewhere. That is, a(n) would be perfect halfband lowpass approximation to x(n).

Of course, in general, a(n) is not going to be equal to x(n). Therefore, we compute the difference between a(n) (our approximation based on y(n)) and x(n).

$$d(n) = x(n) - a(n)$$

It is obvious that x(n) can be reconstructed by adding d(n) and a(n), and the whole process is shown in Fig. 2.3.

In case of a perfect halfband lowpass filter, it is clear that d(n) contains exactly the frequencies above $\pi/2$ of x(n), and thus, d(n) can be subsampled by two as well without loss of information.

The scheme can be iterated on y(n) creating a hierarchy of lower resolution signals at lower scales. Because of that hierarchy and the fact that signals become shorter and shorter, such schemes are called signal pyramids.

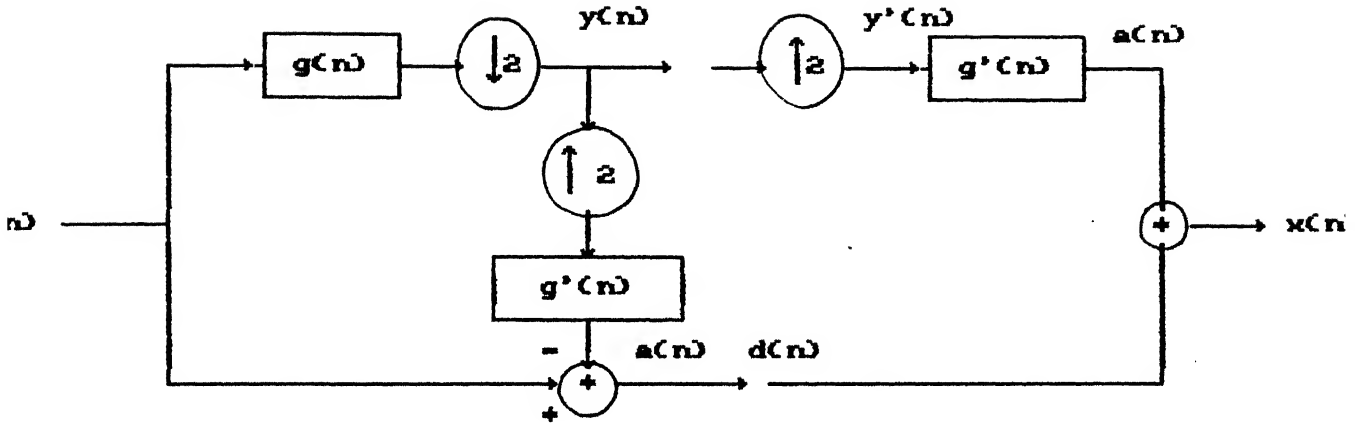

Fig. 2.3 Pyramid scheme. Derivation of lowpass, subsampled approximation y(n), from which an approximation a(n) to x(n) is derived by upsampling and interpolation. Then, the difference between the approximation a(n) and the original x(n) is computed as d(n). Perfect reconstruction is simply obtained by adding a(n) back.

.5 SUB-BAND CODING SCHMES [4]

The above system (pyramid scheme) creates a redundant set of samples, since a signal with sampling rate f_s is mapped to two signals d(n) and y(n) with sampling rates f_s and $f_s/2$ respectively. More precisely, one stage of a pyramid decomposition leads to both a half rate low resolution signal and a full rate difference signal, resulting in an increase in the number of samples by 50%.

Now a different scheme instead, where no such redundancy occurs is looked into. It is the so-called sub-band coding scheme first popularized in speech compression. The lowpass, subsampled approximation is obtained exactly as explained above, but, instead of a difference signal, we compute the "added detail" as a highpass filtered version of x(n) (using a filter with impulse response h(n)) followed by subsampling by two. Intuitively, it is clear that the added detail to the lowpass approximation has to be a highpass signal, and it is obvious that if g(n) is an ideal halfband lowpass filter, then an ideal halfband highpass filter h(n) will lead to a perfect representation of the original signal into two subsampled versions.

This is exactly one step of a wavelet decomposition using sin(x)/x filters; since the original signal is mapped to a lowpass approximation (at twice the scale) and an added detail signal (also at twice the scale). In particular using these ideal

filters, the discrete version is identical to the continuous wavelet transform.

It is not necessary to use ideal (hence impractical) filters and yet x(n) can be recovered from its two filtered and subsampled versions which we now call $y_0(n)$ and $y_1(n)$. To do so, both are upsampled and filtered by g'(n) and h'(n) respectively, and finally added together, as shown in Fig. 2.4. Now unlike the Pyramid case, the reconstructed signal (which we now call $\hat{x}(n)$ is not identical to x(n) unless the filters meet some specific constraints. Filters that meet these constraints are said to have perfect reconstruction property. The easiest case to analyse appears when the analysis and synthesis filters are identical and when perfect reconstruction is achieved i.e. $\hat{x}(n) = x(n)$ within a possible shift. Then it can be shown that the sub-band analysis/ synthesis corresponds to decomposition onto an orthonormal basis, followed by a reconstruction which amounts to summing up the orthgonal projections. FIR filters are assumed. Then it turns out that the highpass and lowpass filters are related by

$$h(L-1-n) = (-1)^n g(n) \qquad (2.34)$$

where L is the filter length. The modulation by $(-1)^n$ transforms the lowpass filters to the highpass one.

2.6 LAPLACIAN PYRAMIDAL MULTIRESOLUTION DECOMPOSITION AND RECONSTRUCTION [1]

The approximation of a signal f(x) at a resolution 'r' is defined as an estimate of f(x) derived from 'r' measurements per

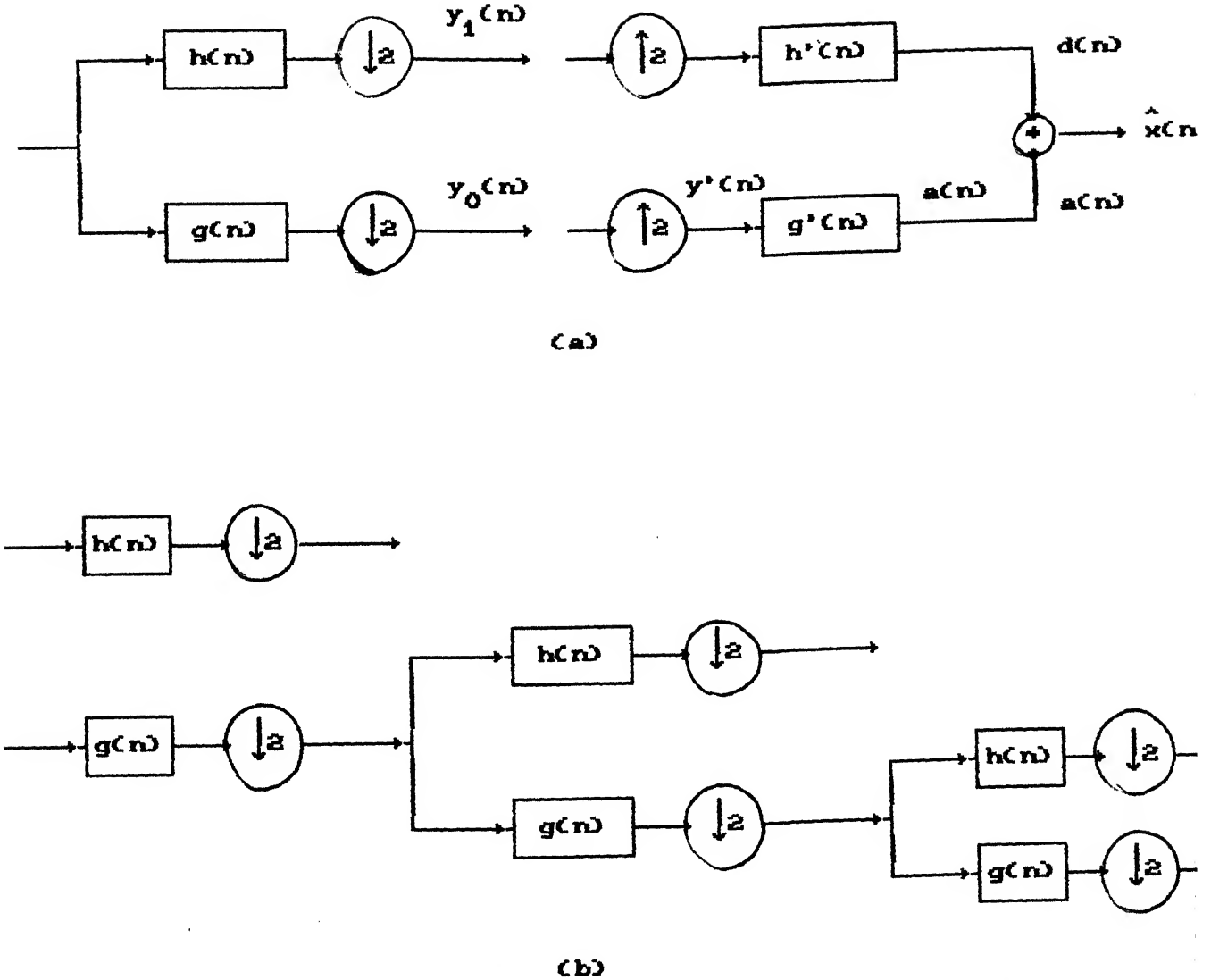

Fig. 2.4 Suband Coding scheme. (a) Two subsampled approximations, one corresponding to low and the other to high frequencies, are computed. The reconstructed signal is obtained by re-interpolating the approximations and summing them. The filters on the left form an analysis filter bank, while on the right is a synthesis filter bank. (b) Block diagram (Filter Bank tree) of the Discrete Wavelet Transform implemented with discrete-time filters and subsampling by two.

unit length. These measurements are computed by uniformly sampling at a rate r the function f(x) smoothed by a lowpass filter whose bandwidth is proportional to r. In order to be consistent when the resolution varies, these lowpass filters are derived from a unique function $\theta(x)$ which is dilated by the resolution factor r : $\theta_r = \sqrt{r}\theta(rx)$. The set of measurements $Arf = (f * \theta_r(n/r))_{n\in Z}$ is called the discrete approximation of f(x) at the resolution r. The discrete approximation of a function f(x) at the resolution 2^j is thus given by

$$A_2 jf = \left[f * \theta_{2^j} \left(\frac{n}{2^j} \right) \right]_{n\in Z} \tag{2.35}$$

In pyramidal multiresolution algorithms, the lowpass filter function $\theta(x)$ is chosen such that its Fourier transform can be written

$$\hat{\theta}(\omega) = \prod_{p=1}^{\infty} U\left[e^{-2i-p\omega}\right] \tag{2.36}$$

where $U(e^{-i\omega})$ is the transfer function of a lowpass discrete filter $U = \left[u_n\right]_{n\in Z}$. Let us suppose that we have already computed the discrete approximation of a function $f(x) \in L^2(R)$ at the resolution 2^{j+1} : $A_2 j+1f = \left[f * \theta_{2^{j+1}} (n/2^{j+1})\right]_{n\in Z}$. The discrete approximation of f(x) at a resolution 2^j is calculated by filtering $A_2 j+1f$ with the discrete lowpass filter $U = \left[u_n\right]_{n\in Z}$ and keeping every other sample of the convolution product.

Let $\Lambda = \left(\lambda_n \right)_{n\in Z}$ be such that

$$\Lambda = A_2 j+1f * U \tag{2.37}$$

then $$A_2 j\ f = \left(\lambda_{2n}\right)_{n\in Z} \tag{2.38}$$

The approximation of this signal at any resolution 2^{-J}, $J>0$, can be computed by iterating on (2.37) and (2.38) and j varying between 0 and J+1. This pyramidal algorithm is illustrated in Fig. 2.5(a). The set of discrete approximations $\left(A_2 jf\right)_{0\geq j\geq -J}$ is called a Gaussian Pyramid.

Now the algorithm by Burt and Crowley is described in order to extract the details of f(x) which appear in $A_2 j+1f$ but not in $A_2 jf$. The discrete approximation $A_2 j+1f$ has twice as many samples as $A_2 jf$, so we first expand $A_2 jf$ by a factor of two. This is done by interpolation. A zero is put between each sample of $A_2 jf$ and filter the resulting signal with a lowpass filter. In this algorithm, the lowpass filter is the filter U defined previously. Let $A_2^e jf$ be the expanded discrete signal. The details $D_2 jf$ at the resolution 2^j are then computed by subtracting $A_2^e jf$ from $A_2 j+1f$.

$$D_2 jf = A_2 j+1f - A_2^e jf \tag{2.39}$$

This algorithm decomposes a discrete approximation $A_1 f$ at the resolution of 1 into an approximation $A_2{-J}\ f$ at a coarse resolution 2^{-J} and the successive detail signals $(D_2 jf)_{0<j\leq -J}$. If the signal $A_1 f$ has N non-zero samples, each detail signal $D_2 jf$ has $2^{j+1}N$ samples; whereas the coarse signal $A_2{-j}f$ has $2^{-j}N$ samples. Hence, the total number of samples of this representation is approximately 2N. The signals $\left\{A_2{-J}f,\ (D_2 jf)_{0<j\leq -J}\right\}$ are regrouped in a data structure called a Laplacian Pyramid.

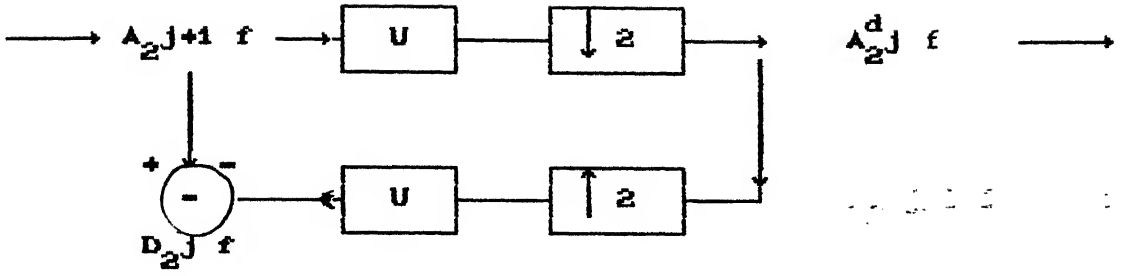

(a)

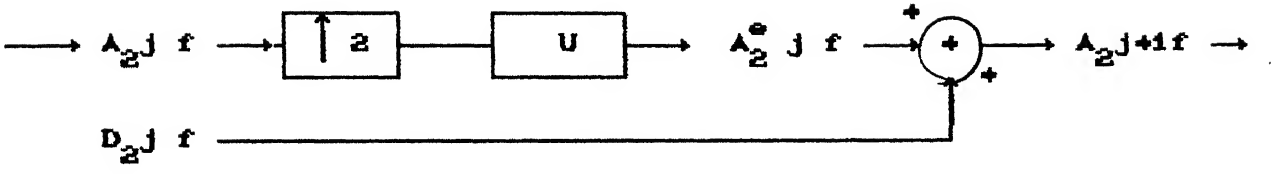

(b)

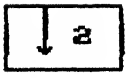

: keep one sample out of two

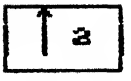

: put a zero between each sample

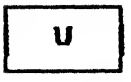

: convolution with the discrete filter U

Fig. 2.5 (a) Decomposition of $A_2 j+1\ f$ into $A_2 j\ f$ and $D_2 j\ f$ when computing a Laplacian pyramid (b) Reconstruction of $A_2 j+1\ f$ from $A_2 j\ f$ and $D_2 j\ f$ when reconstructing the original signal from a Laplacian Pyramid Scheme.

The original signal can easily be reconstructed from such a decomposition. At each resolution, we compute $A_2 j+1 f$ by expanding the details $D_2 jf$. By repeating this algorithm when j is varying between -J and 0, we reconstruct $A_1 f$. The reconstruction algorithm is illustrated by a block diagram in Fig. 2.5(b) [1].

2.7 COMPARISON BETWEEN SHORT TIME FOURIER TRANSFORM AND WAVELET TRANSFORM

2.7.1 Short Time Fourier Transform (STFT) as Window Fourier Transform [1] & [4]

From the Fourier Transform of a function f(x), we get a measure of the irregularities (high frequencies) but this information is not spatially localized. Indeed, the Fourier transform $\hat{f}(\omega)$ is defined through an integral which covers the whole spatial domain. It is therefore difficult to find the position of the irregularities. In order to localize the information provided by the Fourier Transform, Fabor defined a new decomposition using a spatial window g(x) in the fourier integral. This window is translated along the spatial axis in order to cover the whole signal. At a position u and for a frequency ω, the window fourier transform of a function $f(x) \in L^2(R)$ is defined by

$$Gf(\omega,u) = \int_{-\infty}^{\infty} e^{-i\omega x}\, g(x-u)\, f(x)\, dx. \qquad (2.40)$$

If measures, locally around the point u, the amplitude of the sinusoidal wave component of the frequency ω. In the original Gabor transform, the window function g(x) is a Gaussian. It has seen been generalized for any type of window function and is called a window Fourier Transform. The window function is generally a real even function and the energy of its Fourier Transform is concentrated in the low frequencies [1]. It can be viewed as the impulse response of a lowpass filter. A window Fourier Transform can also be interpreted as the inner products of the function f(x) with the family of functions $(g\omega,u(x))(\omega,u)\in R^2$.

$$Gf(\omega,u) = \langle f(x), g_{\omega,u}(x) \rangle \tag{2.41}$$

In quantum physics, such a family of functions is called a family of coherent states. The Fourier Transform $g_{\omega,u}(x)$ is given by

$$\hat{g}_{\omega_0 u_0}(\omega) = e^{-iu_0\omega}\,\hat{g}(\omega - \omega_0) \tag{2.42}$$

where $\hat{g}(\omega)$ is the Fourier transform of g(x). A family of coherent states thus corresponds to a translation in the spatial domain (parameter u) and in the frequency domain (parameter ω) of the function g(x). This double translation is represented in phase-space where one axis corresponds to the spatial parameter u and the other to the frequency parameter ω (Fig. 2.6). Familiies of coherent states have found many applications in quantum physics

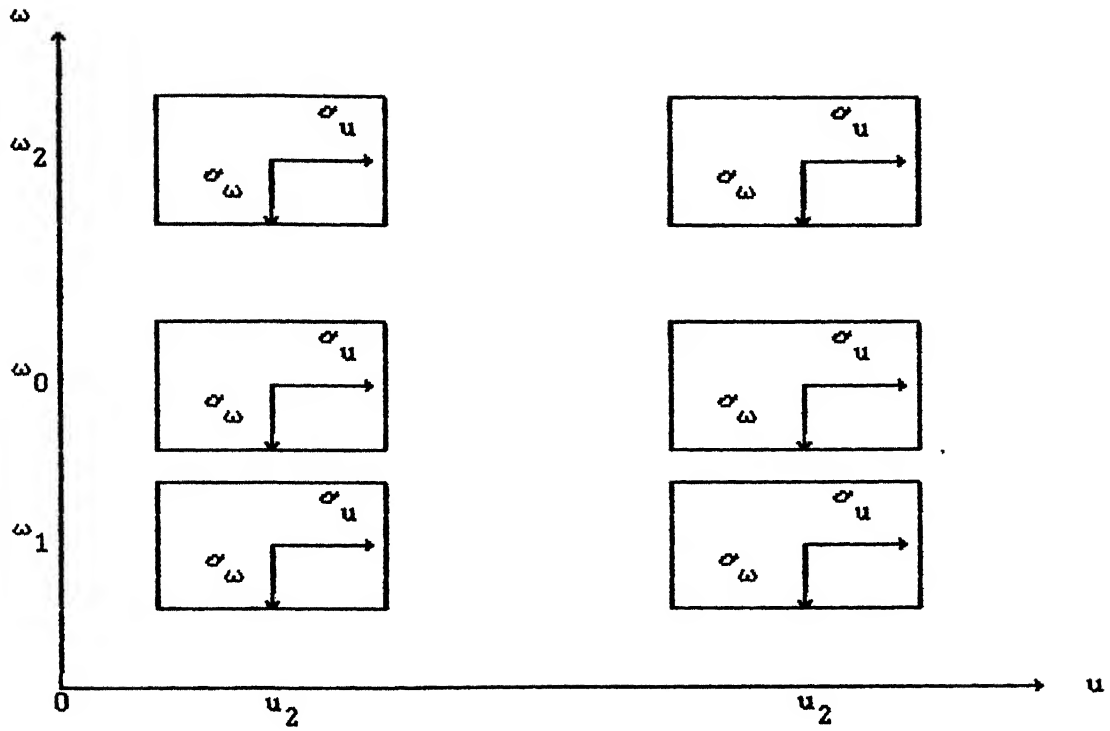

Fig. 26 Phase-space representation. The vertical axis gives the frequency ω whereas the horizontal axis gives the spatial position u. A window Fourier coefficient $Gf(\omega_0,u_0)$ provides a description of f(x) within the resolution cell of $[u_0 - \sigma_u, u_0 + \sigma_u] \times [\omega_0 - \sigma_\omega, \omega_0 + \sigma_\omega]$

because they make it possible to analyze simultaneously a physical phenomena in both the spatial and frequency domains.

Let us now describe how a window Fourier transform relates to a spatial or a frequency representation. Let σ_u be the standard deviation of $g(x)$

$$\sigma_u^2 = \int_{-\infty}^{+\infty} x^2 \, |g(x)|^2 \, dx \tag{2.43}$$

Let σ_ω be the standard deviation of the Fourier transform of $g(x)$

$$\sigma_\omega^2 = \int_{-\infty}^{+\infty} \omega^2 \, |\hat{g}(\omega)|^2 \, d\omega \tag{2.44}$$

The function $g_{\omega_0,u_0}(x)$ is centered in u_0 and has a standard deviation of σ_u in the spatial domain. Its Fourier transform given by (2.42) is centered in ω_0 and has a standard deviation σ_ω. By applying the Parseval theorem on (2.41), we get

$$\begin{aligned} Gf(\omega_0,u_0) &= \int_{-\infty}^{+\infty} f(x) \, \overline{g_{\omega_0,u_0}(x)} \, dx \\ &= \int_{-\infty}^{+\infty} \hat{f}(\omega) \, \overline{g_{\omega_0,u_0}(\omega)} \, d\omega \; . \end{aligned} \tag{2.45}$$

The first integral shows that in the spatial domain, $Gf(\omega_0,u_0)$ essentially depends upon the values of $f(x)$ for $x \in \left[u_0-\sigma_u, u_0+\sigma_u\right]$. The second integral proves that in the frequency domain, $Gf(\omega_0,u_0)$ depends upon the values of $\hat{f}(\omega)$ for $\omega \in \left[\omega_0-\sigma_\omega, \omega_0+\sigma_\omega\right]$.

The spatio-frequency domain which is covered by $Gf(\omega_0,u_0)$ can thus be represented in the phase-space by the resolution cell $\left[u_0-\sigma_u,u_0+\sigma_u\right] \times \left[\omega_0-\sigma_\omega,\omega_0+\sigma_\omega\right]$ as shown in Fig. (2.6). The surface and shape of the resolution cell is independent from u_0 and ω_0. The uncertainty principle applied to the function g(x) implies that

$$\sigma_u^2 \, \sigma_\omega^2 \geq \frac{\pi}{2} \tag{2.46}$$

The resolution cell can therefore not be smaller than $2\sqrt{2\pi}$. The uncertainty inequality reaches its upper limit if and only if g(x) is a Gaussian. Hence, the resolution in the phase-space is maximimized when the window function is a Gaussian as in the Gabor transform.

The STFT maps the signal into a two-dimensional function in a time-frequency plane (ω,u). It can also be viewed as follows. At a given frequency ω, the STFT amounts to filtering the signal 'at all times', with a bandpass filter having as impulse response the window function modulated to that frequency. Given a window function g(x) and its Fourier transform $G(\omega)$, define the bandwidth $\Delta\omega$ of the filter as

$$\Delta\omega^2 = \frac{\int \omega^2 \, |G(\omega)|^2 \, d\omega}{\int |G(\omega)|^2 \, d\omega} \tag{2.47}$$

where the denominator is the energy of the g(x). Two sinusoids will be discriminated if they are more that $\Delta\omega$ apart. Thus, the

resolution in frequency is given by Δf. Similarly, the spread in time is given by Δx as

$$\Delta x^2 = \frac{\int x^2 \, |g(x)|^2 \, dx}{\int |g(x)|^2 \, dx} \qquad (2.48)$$

where the discrimator is again the energy of g(x). Two pulses in time can be discriminated only if they are more than Δx apart.

Now resolution in time and frequency cannot be arbitrarily small, because their product is lower bounded.

$$\text{Time-bandwidth product} = \Delta x \, \Delta \omega \geq \frac{1}{4\pi}$$

This is referred to as the uncertainty principle or Heisenberg inequality [4]. It means that one can only trade time resolution for frequency resolution, or vice-versa. Gaussian windows are therefore often used since they meet the bound with equality.

2.7.1 Wavelet Transform [1]

Morlet defined the wavelet transform by decomposing the signal into a family of functions which are the translation and dilation of a unique function $\psi(x)$. The function $\psi(x)$ is called a wavelet and the corresponding wavelet family is given by $(\sqrt{s}\psi(s(x-u))_{s,u \in R}{}^2$. The wavelet transform of a function $f(x) \in L^2(R)$ is defined by

$$Wf(s,u) = \int_{-\infty}^{\infty} f(x) \sqrt{s} \, \psi(s(x-u)) \, dx \qquad (2.49)$$

Let us denote the dilation of $\psi(x)$ with a factor s by

$$\psi_s(x) = \sqrt{s}\ \psi\ (sx)$$

A wavelet transform can be rewritten as inner products in $L^2(R)$

$$Wf.(s,u) = \langle\ f(x),\ \psi_s(x-u)\ \rangle \qquad (2.50)$$

It thus corresponds to a decomposition of f(x) on the family of functions $\left[\psi_s(x-u)\right]_{s,u\in R^2}$. The functions $\psi_s(x)$ have the same type as $\psi(x)$, but have a support s times smaller. If wavelet $\psi(x)$ and signal f(x) have real values, in order to reconstruct f(x) from its wavelet transform, the Fourier Transform $\hat{\psi}(\omega)$ of $\psi(x)$ must satisfy

$$C\psi = \int_{-\infty}^{\infty} \frac{|\ \hat{\psi}(\omega)|^2}{\omega}\ ds \quad <+\infty \qquad (2.51)$$

The function $\psi(x)$ can be interpreted as impulse response of a bandpass filter. Let us denote $\hat{\psi}_s(x) = \psi_s(-x)$. We can rewrite the wavelet transform at a point u and a scale s as a convolution product with $\hat{\psi}_s(x)$

$$Wf\ (s,u) \ = \ f\ *\ \hat{\psi}_s(u)\ . \qquad (2.52)$$

A wavelet transform can therefore be viewed as a filtering of f(x) with a bandpass filter whose impulse response is $\hat{\psi}_s(x)$. The fourier transform of $\psi_s(x)$ is given by

$$\hat{\psi}_s(\omega) \ = \ \frac{1}{\sqrt{s}}\ \hat{\psi}\ (\omega/s) \qquad (2.53)$$

In opposition to a window Fourier transform which has a fixed resolution in the spatial and frequency domain, the resolution of a Wavelet Transform varies with the scale parameter s. Since $\psi(x)$ is real, $|\hat{\psi}(\omega)| = |\hat{\psi}(-\omega)|$. Let us ω_o the centre of the passing band of $\hat{\psi}(\omega)$

$$\int_0^\infty (\omega-\omega_o) \, |\hat{\psi}(\omega)|^2 \, d\omega = 0 \qquad (2.54)$$

Let σ_ω be the rms bandwidth around ω_o

$$\sigma_\omega^2 = \int_0^\infty (\omega-\omega_o) \, |\hat{\psi}(\omega)|^2 \, d\omega. \qquad (2.55)$$

It is clear that centre of the passband of $\hat{\psi}_s(\omega)$ is $s\omega_o$ and that its r.m.s bandwidth is $s\sigma\omega$. On a logarithmic scale, the rms bandwidth of $\hat{\psi}_s(\omega)$ is the same for all $s \in R^+$. Hence a wavelet transform decomposes the signal into a set of frequency bands having a constant size on a logarithm scale.

Let σ_u be the standard deviation of $|\psi(x)|^2$ around zero. One can also show easily that the wavelet $\psi_s(x - u_0)$ has an energy concentrated around u_0 within a standard deviation σ_u/s. In the frequency domain, we saw that its energy is concentrated around $s\omega_0$ within a standard deviation $s\sigma_\omega$. In the phase-space, the resolution cell of this wavelet is therefore equal to $[u_0-\sigma_u/s)$, $u_0 + (\sigma_u/s)] \times [s\omega_0 - s\sigma_\omega, s\omega_0 + s\sigma_\omega]$. As opposed to a window Fourier transform, the shape of the resolution cell varies with

the scale s. This is illustrated in Fig. 2.7. When the scale s is small, the resolution is coarse in the spatial domain and fine in the frequency domain. If the scale s increases, the resolution increases in the spatial domain and decreases in the frequency domain (Fig. 2.7).

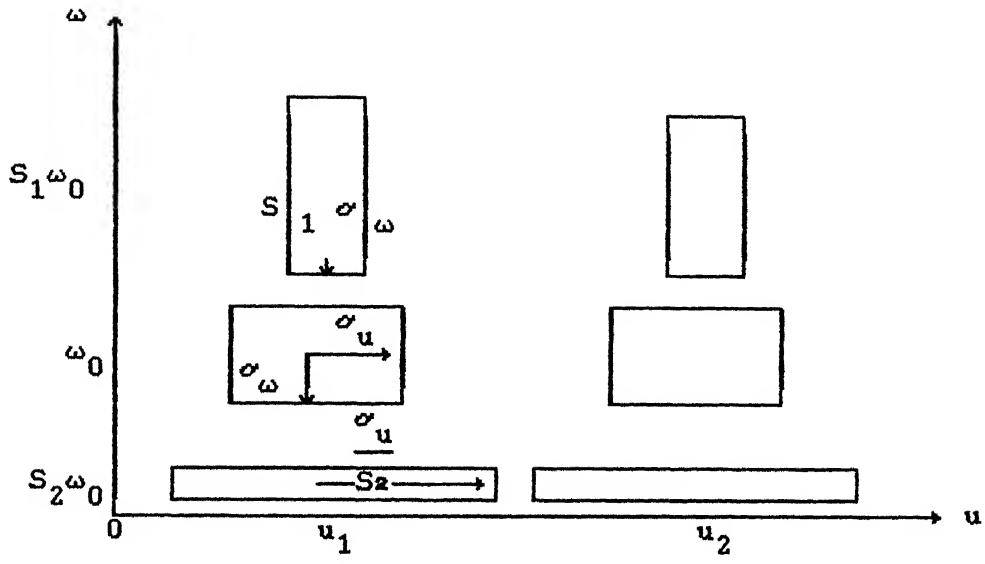

Fig. 2.7 In the phase-space, the shape of a wavelet resolution cell depends upon the scale. When the scale increases, the resolution increases in the spatial domain and decreases in the frequency domain. The surface of all the resolution cell is the same.

CHAPTER - 3

RESULTS

3.1 DESIGN OF WAVELETS

The wavelet functions $\psi(x)$ have been constructed from orthogonal basis functions. Amongst the known orthogonal basis functions are Linear Spline, Haar basis, Quadratic Spline, and Cubic Spline.

We start with a function ϕ such that ϕ_{on} are an orthonormal basis for V_0. Since $\phi \in V_0 \subset \text{span} \left\{\phi(2.-n)\right\}$ there exists C_n such that

$$\phi(x) = \sum_n C_n \phi(2x-n) \tag{3.1}$$

Define then

$$\psi(x) = \sum_n (-1)^n C_{n+1} \phi(2x+n) \tag{3.2}$$

Then $\left\{\psi_{mn},\ m,n \in Z\right\}$ constitute an orthonormal basis of wavelets for $L^2(R)$.

Now we take up orthogonal basis functions one by one.

3.1.1 Haar Basis [3]

The orthogonal function is given by

$$\phi(x) = \begin{cases} 1 & 0 \le x < 1 \\ 0 & \text{Otherwise} \end{cases}$$

$\phi(x)$ is also expressed as

$$\phi(x) = \phi(2x) + \phi(2x-1) \tag{3.3}$$

Since $\phi(x) = C_0\phi(2x) + C_1\phi(2x-1)$

Therefore,

$$C_0 = 1, \quad C_1 = 1.$$

By equation (3.2),

$$\psi(x) = \phi(2x) - \phi(2x-1) \tag{3.4}$$

Hence

$$\psi(x) = \begin{cases} 1 & 0 \le x \le 1 \\ -1 & 1/2 \le x < 1 \\ 0 & \text{Otherwise.} \end{cases}$$

3.1.2 Linear Spline [3]

The function is given as

$$\phi(x) = \begin{cases} x & 0 \le x \le 1 \\ 2-x & 1 \le x \le 2 \\ 0 & \text{Otherwise.} \end{cases}$$

$\phi(x)$ is also expressed as

$$\phi(x) = \frac{1}{2}\phi(2x) + \phi(2x-1) + \frac{1}{2}\phi(2x-2) \tag{3.5}$$

Hence $C_0 = \frac{1}{2}$, $C_1 = 1$, $C_2 = \frac{1}{2}$

By equation (3.2)

$$\psi(x) = -\frac{1}{2}\phi(2x+1) + \phi(2x) - \frac{1}{2}\phi(2x-1) \qquad (3.6)$$

Hence

$$\begin{aligned}
\psi(x) &= -(x + \tfrac{1}{2}) && -\tfrac{1}{2} \le x \le 0 \\
&= (3x - \tfrac{1}{2}) && 0 \le x \le \tfrac{1}{2} \\
&= (\tfrac{3}{2} - x) && \tfrac{1}{2} \le x \le 1 \\
&= (\tfrac{3}{2} - x) && 1 \le x \le \tfrac{1}{2}
\end{aligned}$$

3.1.3 Quadratic Spline

The quadratic spline function is given by

$$\begin{aligned}
\phi(x) &= x^2 && 0 \le x \le 1 \\
&= -2x^2+6x-3 && 1 \le x \le 2 \\
&= (3-x)^2 && 2 < x \le 3 \\
&= 0 && \text{Otherwise.}
\end{aligned}$$

$\phi(x)$ is also expressed as

$$\phi(x) = \frac{1}{4}\phi(2x) + \frac{3}{4}\phi(2x-1) + \frac{3}{4}\phi(2x+2) + \frac{1}{4}\phi(2x-3)$$

Hence

$$C_0 = \frac{1}{4}, \quad C_1 = \frac{3}{4}, \quad C_2 = \frac{3}{4}, \quad C_3 = \frac{1}{4}$$

By equation (3.2)

$$\psi(x) = \frac{1}{4}\phi(2x+2) - \frac{3}{4}\phi(2x+1) + \frac{3}{4}\phi(2x) + \frac{1}{4}\phi(2x-1)$$

Hence

$$\psi(x) = -\frac{1}{4}(2x+2)^2 \qquad -1 \le x \le -\frac{1}{2}$$
$$= -5x^2 - 4x - \frac{1}{2} \qquad -\frac{1}{2} \le x \le 0$$
$$= 10x^2 - 4x - \frac{1}{2} \qquad 0 \le x \le \frac{1}{2}$$
$$= -10x^2 + 16x - \frac{11}{2} \qquad \frac{1}{2} \le x \le 1$$
$$= 5x^2 - 14x + \frac{19}{2} \qquad 1 \le x \le \frac{3}{2}$$
$$= (4 - 2x)^2 \qquad \frac{3}{2} \le x \le 2.$$

3.2 DESIGN OF FILTERS

h(n) is the impulse response of discrete filter H. expressed as

$$h(n) = \frac{1}{2}\int \phi\,(x/2).\phi\,(x-n)\,dx.$$

3.2.1 Haar Basis

For the haar basis function, h(n)'s has been calculat tabulated.

Table 3.1

n	h(n)
0	0.5
1	0.5

3.2.2 Linear Spline

For the linear spline function, h(n)'s have been calc and are as follows.

Table 3.2

n	h(n)
0	0.25
1	0.416
2	0.25
3	0.041
-1	0.041

3.2.3 Quadratic Spline

For the quadratic spline function, h(n)'s have been calculated and are as follows :

Table 3.3

n	h(n)
0	0.637
1	-1.729
2	-3.479
3	-5.625
4	0.1208
5	0.004
-1	1.995
-2	0.004

3.2.4 Cubic Spline

The values of h(n)'s are as follows [2] :

n	h(n)	n	h(n)
0	0.542	6	0.012
1	0.307	7	-0.013
2	-0.035	8	0.006
3	-0.078	9	0.006
4	0.023	10	-0.003
5	-0.030	11	-0.002

3.3 TRANSFER FUNCTIONS - FILTERS

The transfer function of the filters H & G corresponding to Haar basis and linear spline has been found out and are plotted (Figs. 3.1 and 3.2). The nature of the filters is highpass and lowpass respectively.

3.4 DECOMPOSITION AND RECONSTRUCTION BY WAVELET TRANSFORM

3.4.1

(i) Exponential :

We have taken a signal, which is as follows :

$$f(x) = 2 \exp\left[-\frac{x}{10}\right] + 2 \exp\left[-\frac{x}{100}\right]$$

This signal was sampled and was then decomposed using the iterative method mentioned in Fig. 2.1. After the decomposition, the signal was reconstructed back by using reverse iterative

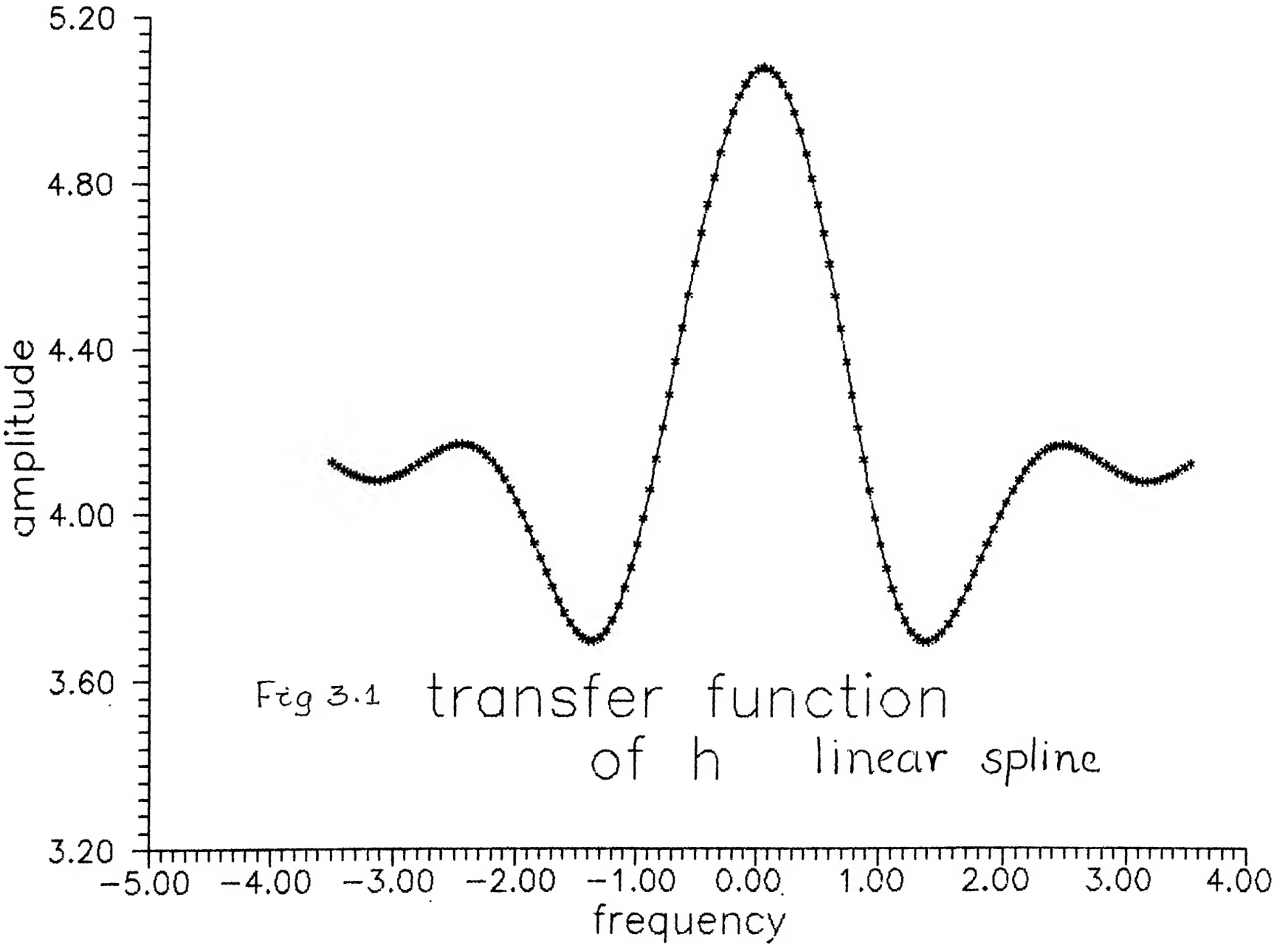

Fig 3.1 transfer function of h linear spline

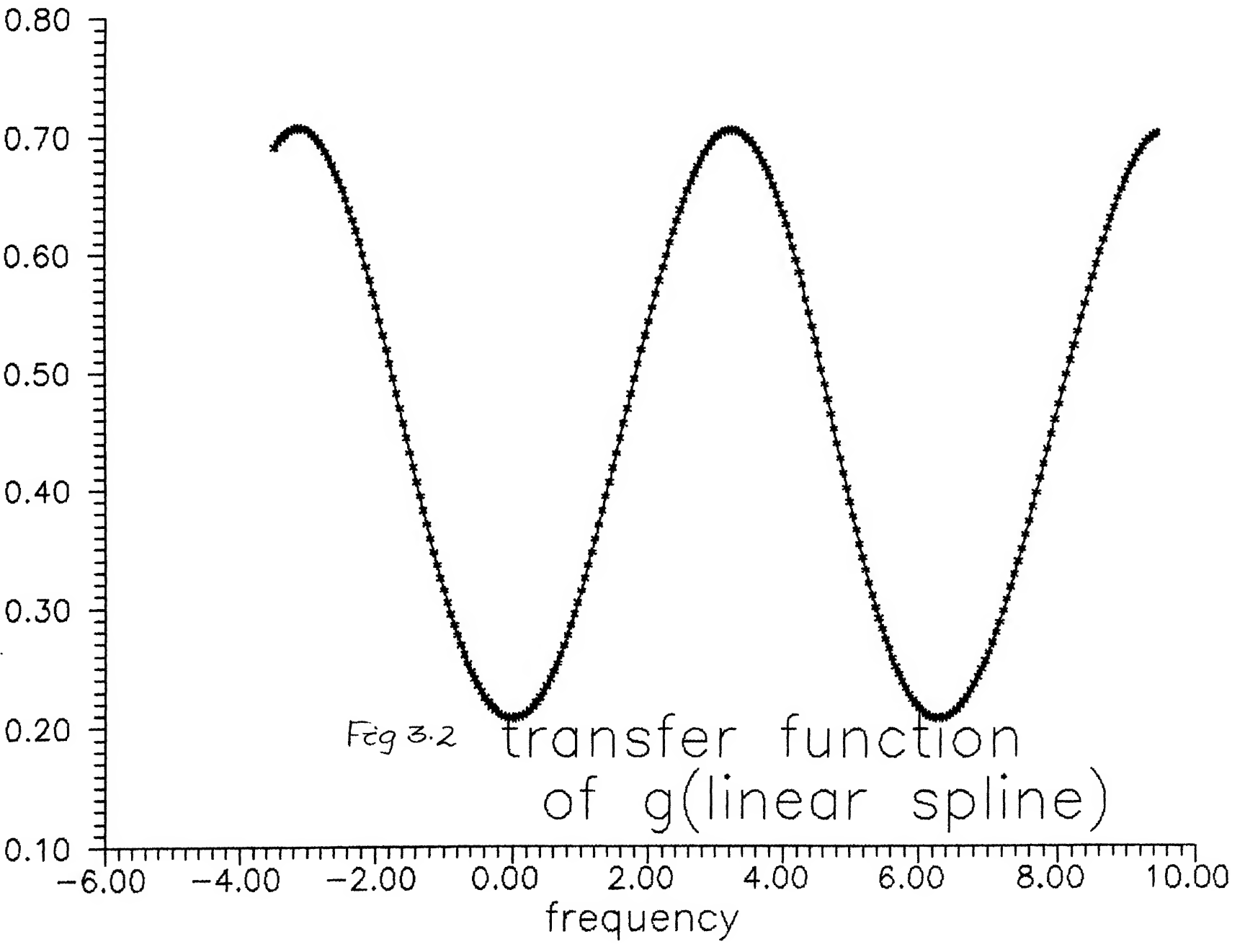

Fig 3.2 transfer function of g(linear spline)

method mentioned in the Fig. 2.2. These procedures were carried out by taking the filters H & G corresponding to cubic spline and linear spline into account (Figs. 3.3 and 3.4).

In both the cases, the reconstructed waveform follows the original waveform i.e. the reconstructed waveform has also an exponential decay.

In case of cubic spline, the reconstructed waveform has some oscillations before they die down to zero. This may be due to the interpolation which is done during the reconstruction of the signal.

In case of Linear Spline there is a sudden dip at the beginning in the reconstructed waveform. This may be due to the nature of the orthogonal basis function which decides the impulse response of the filters.

(ii) Sinusoidal :

We have taken a sinusoidal signal which is as follows

$$f(x) = 2 \exp(-2ix) + \exp(-ix) + 0.5 \exp(-0.5\, ix)$$

The signal was sampled and was decomposed and reconstructed by utilising filters of cubic spline and linear spline (Figs. 3.5 and 3.6). In both the cases, although the reconstructed waveform does follow, the original waveform, but there are irregularities, the reasons again may be due to the interpolation.

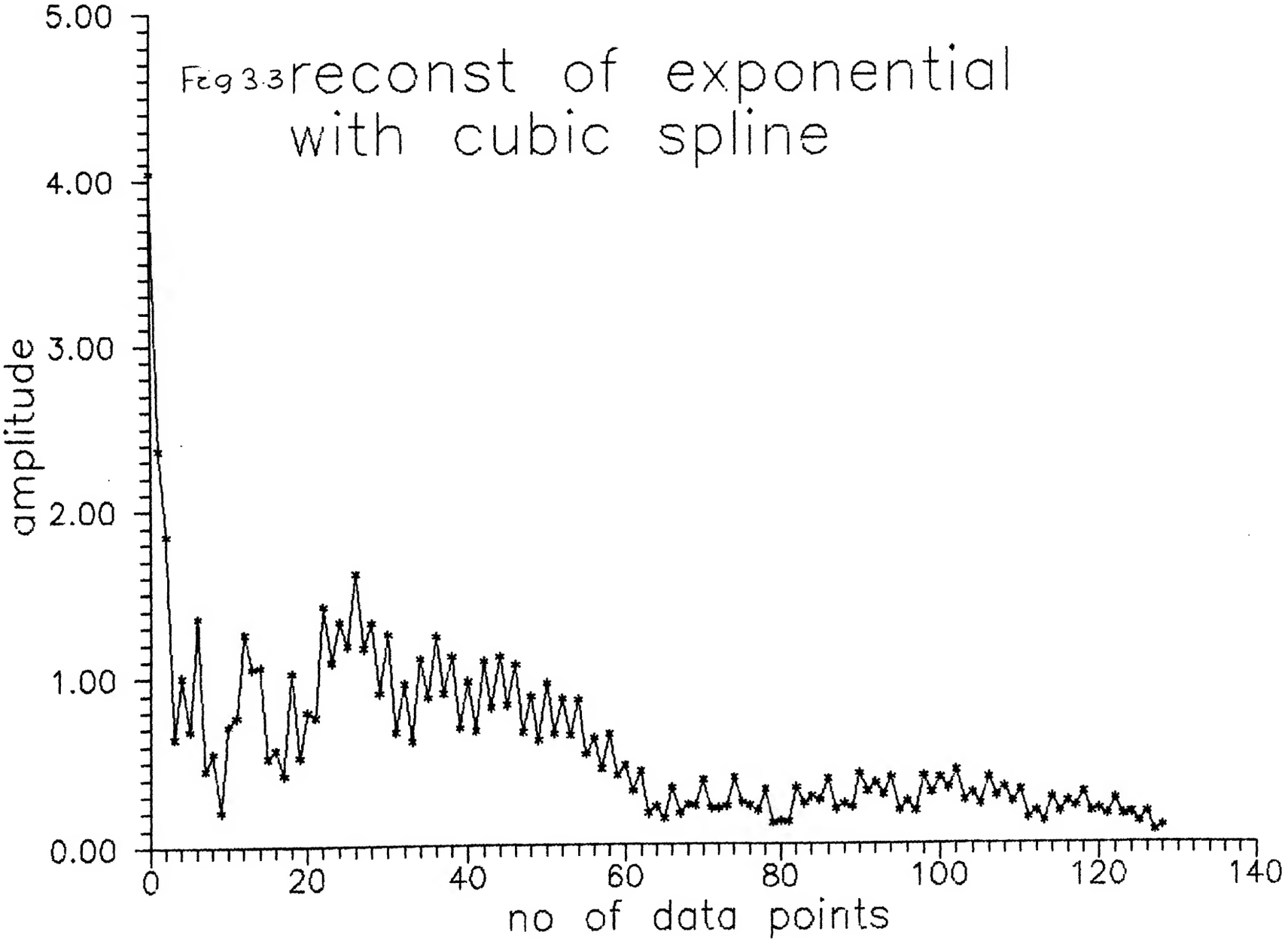
Fig 3.3 reconst of exponential
with cubic spline
5.00
4.00
3.00
2.00
1.00
0.00
amplitude
0
20
40
60
80
100
120
140
no of data points

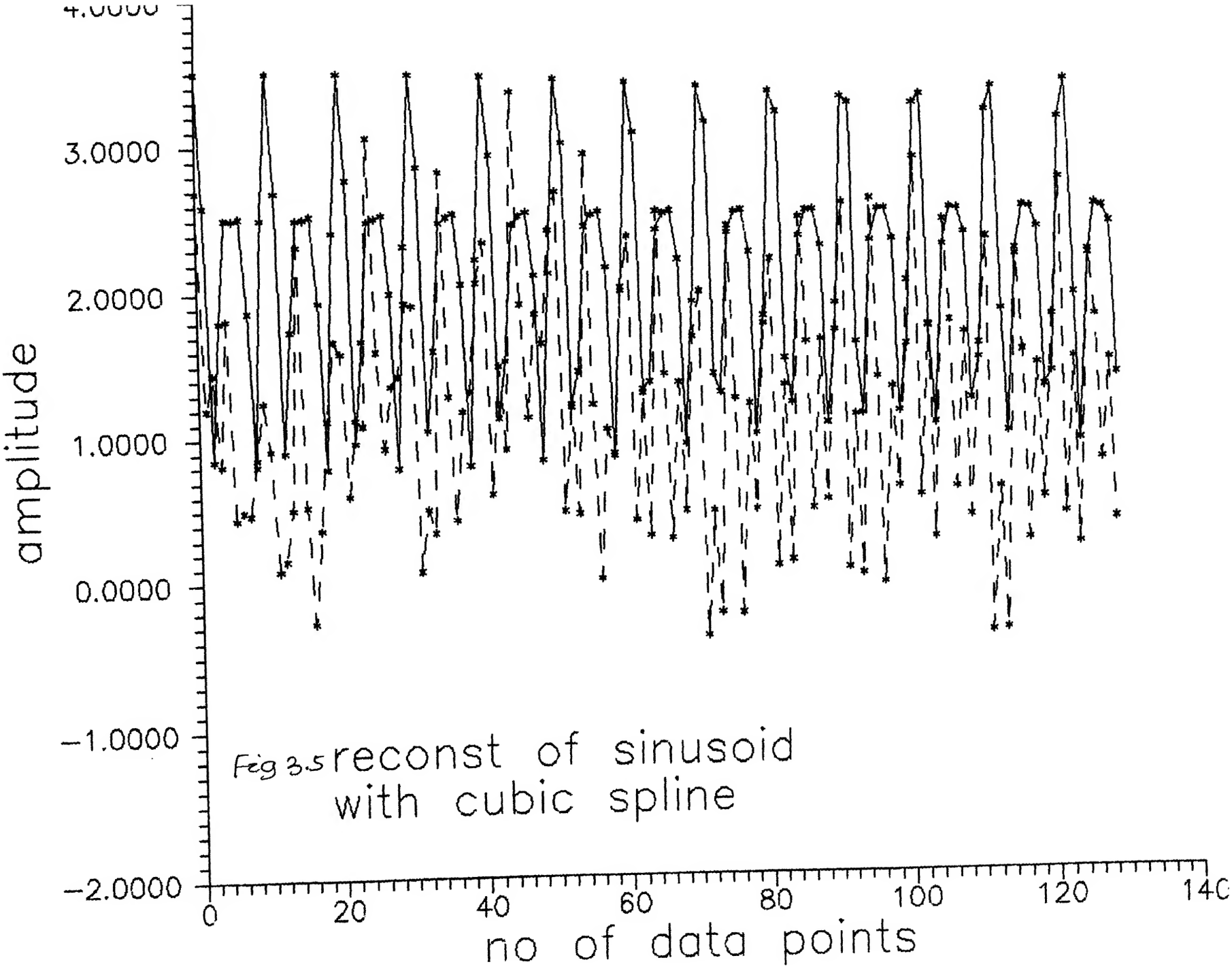

Fig 3.5 reconst of sinusoid with cubic spline

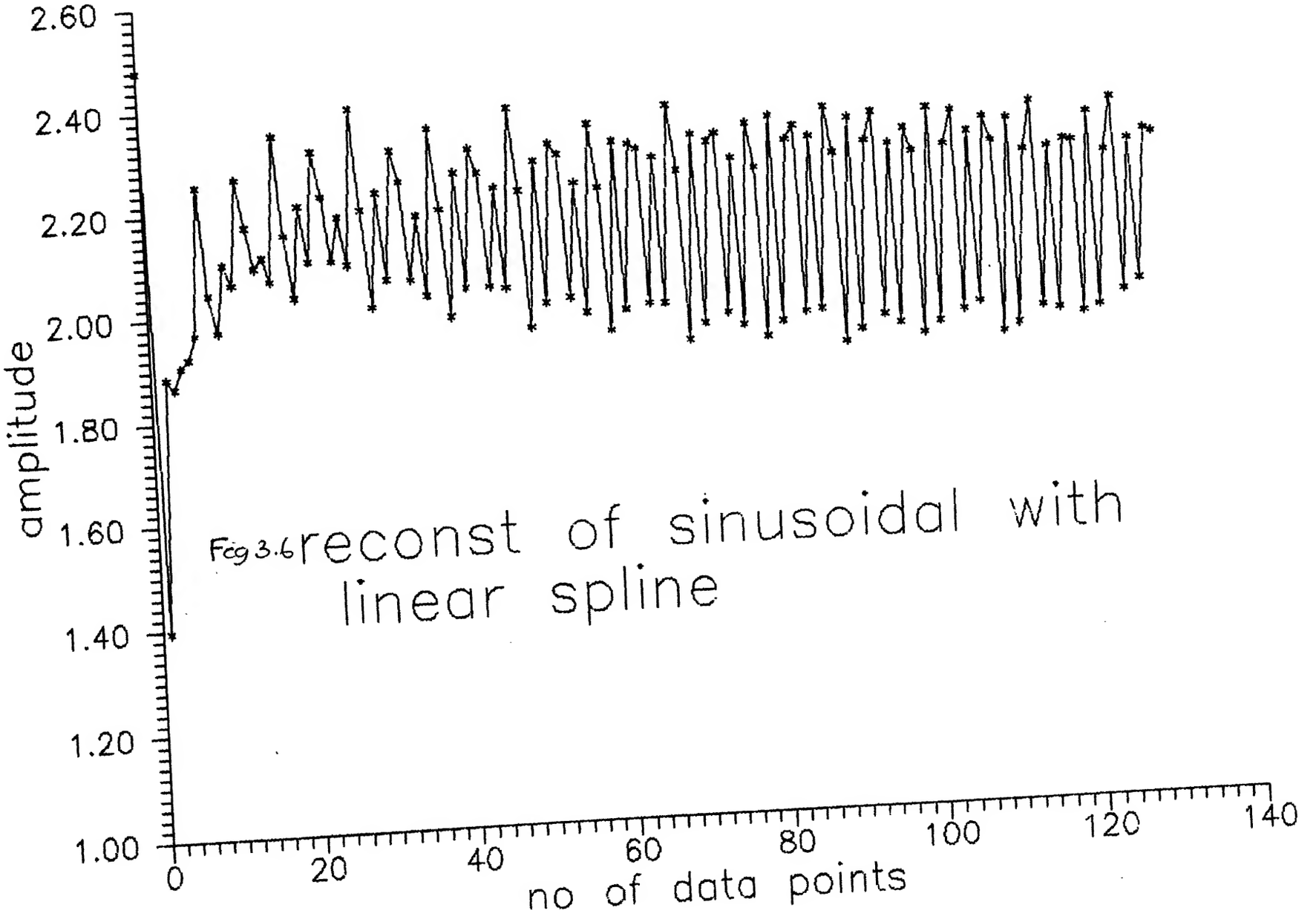

Fig 3.6 reconst of sinusoidal with linear spline

3.4.2 DECOMPOSITION AND RECONSTRUCTION OF SIGNALS WITH NOISE USING WAVELET TRANSFORM

Signals, both exponential as well as sinusoidal were analysed by adding white gaussian noise. The purpose of the adding noise and then reconstructing the signal from its decomposed components is to see whether or not there is an improvement in the signal quality.

(i) **Exponential :**

(a) Cubic Spline : The decomposition and reconstruction of noisy exponential signal was done by using filters based on cubic spline. It was observed that there was no improvement in the signal (Fig. 3.7).

(b) Linear Spline : When filters of linear spline were used, there was improvement of the signal quality. The reconstructed curve, although has a dip at the beginning, is smoother than the original noisy signal (Fig. 3.8).

(ii) **Sinusoidal :**

In case of a noisy sinusoidal signal, the signal quality is not improved compared to the original noisy signal using cubic spline as orthogonal basis function (Fig. 3.9).

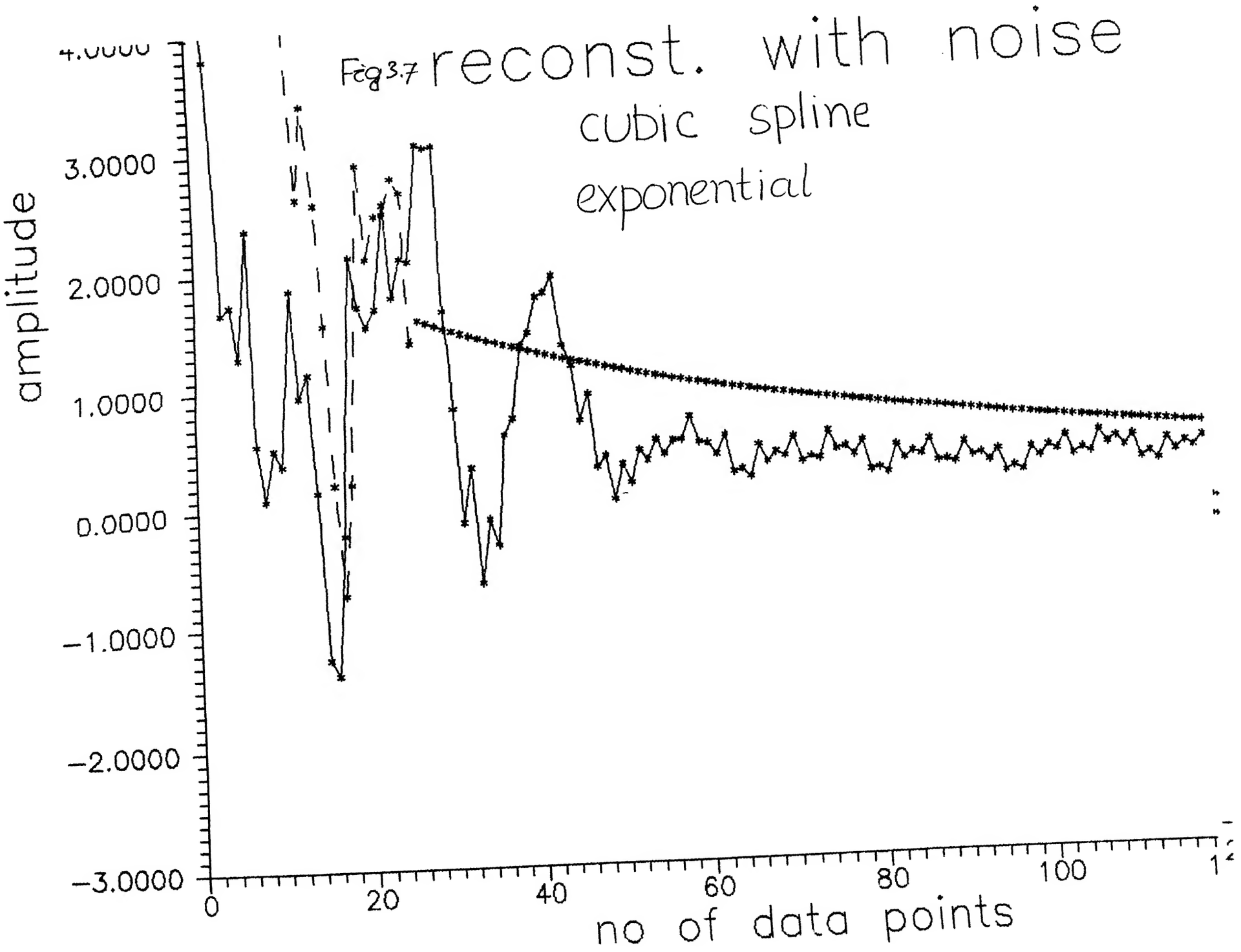
Fig 3.7 reconst. with noise
cubic spline
exponential
amplitude
3.0000
2.0000
1.0000
0.0000
−1.0000
−2.0000
−3.0000
0
20
40
60
80
100
no of data points

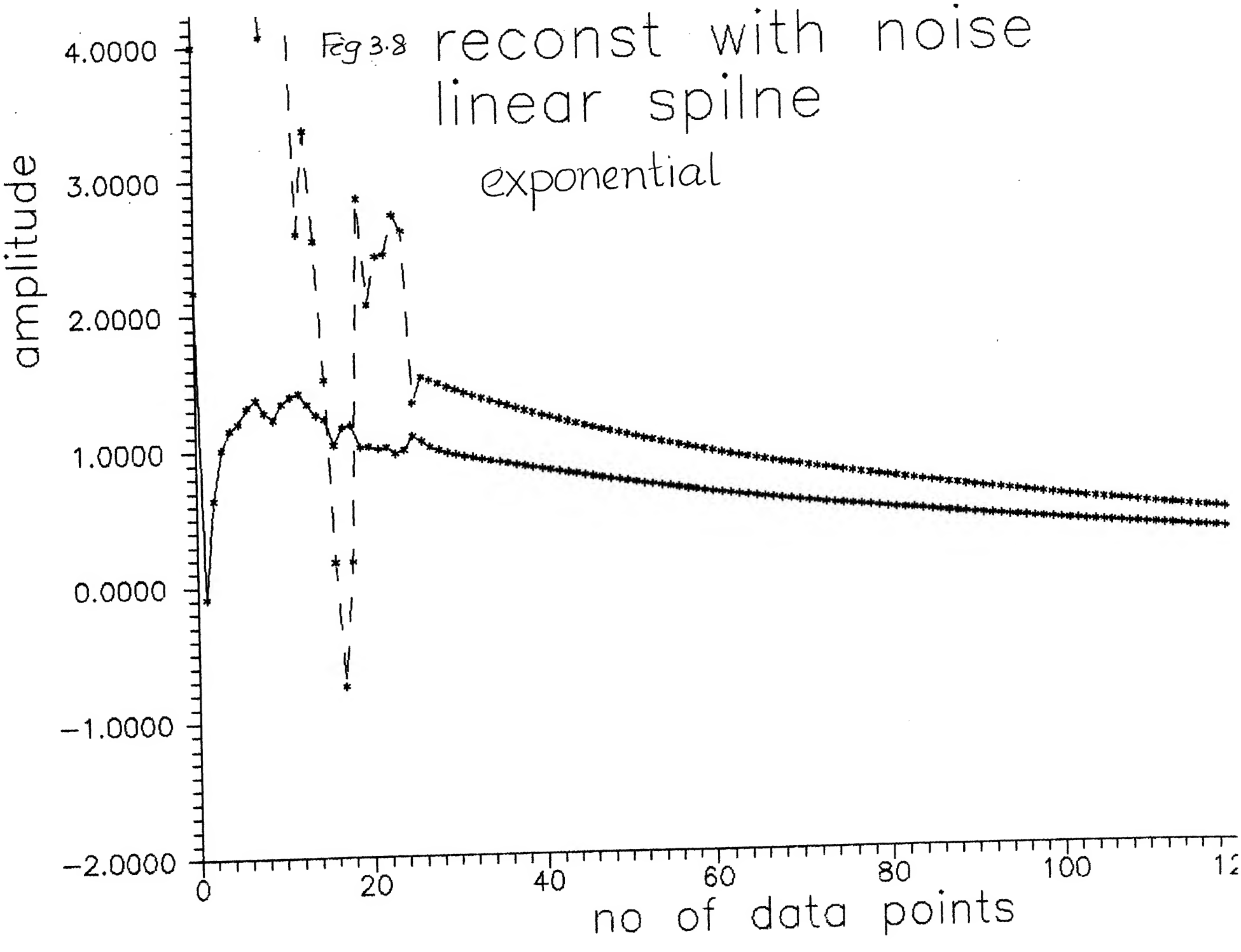
Fig 3.8 reconst with noise
linear spilne
exponential
amplitude
4.0000
3.0000
2.0000
1.0000
0.0000
−1.0000
−2.0000
0
20
40
60
80
100
no of data points

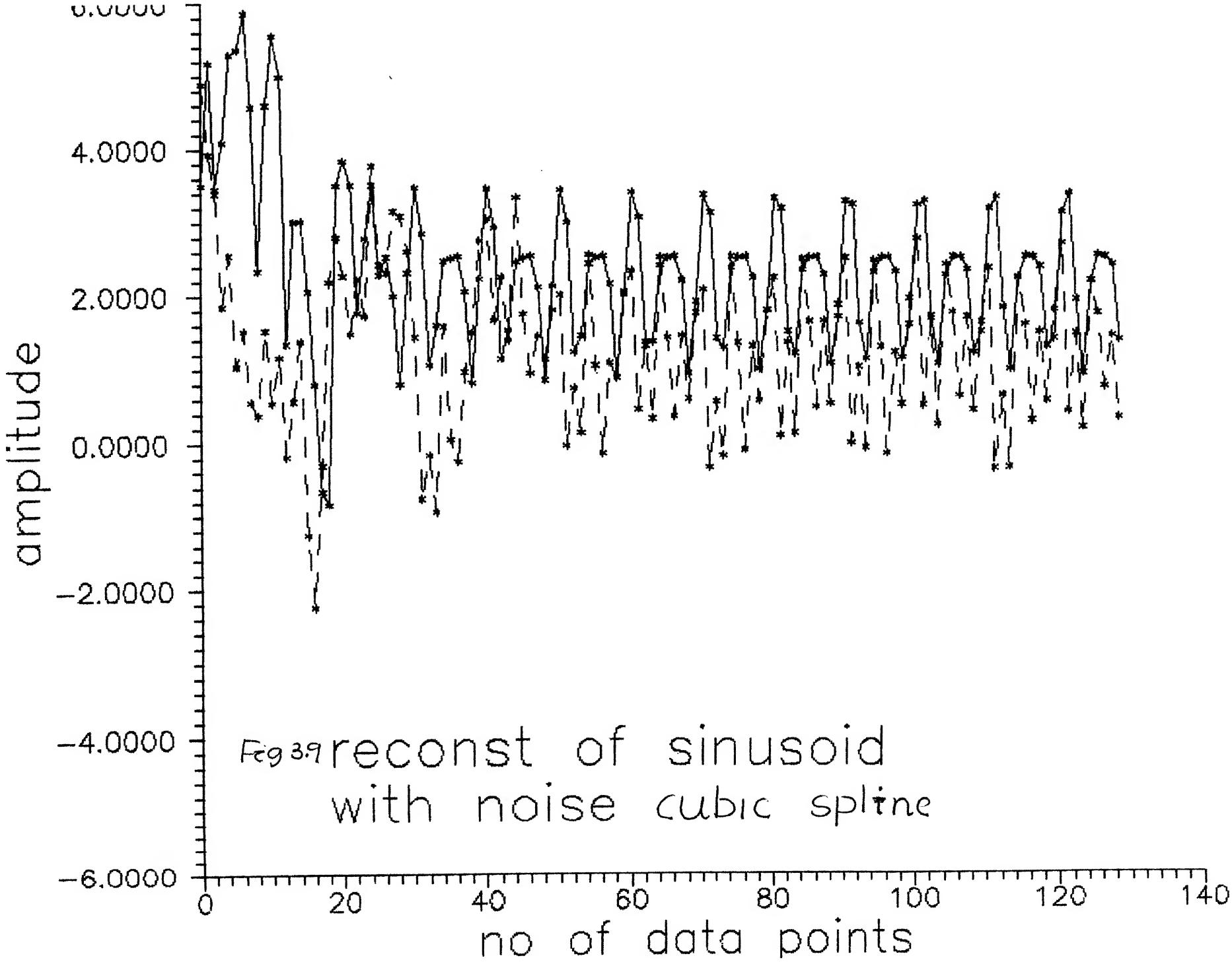

Fig 3.9 reconst of sinusoid with noise cubic spline

3.4.3 DECOMPOSITION AND RECONSTRUCTION OF SIGNAL WITH SPIKES

(i) Exponential

The exponential signal with very closely spaced spikes was taken for analysis. This signal was decomposed and reconstructed with cubic spline and linear spline. It was found out that in the reconstructed signal the spikes were resolved (Figs. 3.10, 3.11 and 3.12).

(ii) Sinusoidal

The sinusoidal signal with closely spaced spikes was also taken for analysis, It was decomposed and reconstructed using cubic spline. The reconstructed signal showed the spikes to have been resolved (Fig. 3.13).

3.5 DECOMPOSITION AND RECONSTRUCTION BY LAPLACIAN PYRAMID SCHEME

The above waveforms have also been decomposed and reconstructed by using Laplacian Pyramid scheme.

(i) Exponential :

The exponential signal when decomposed and reconstructed with the help of Laplacian Pyramid Scheme, does follow the original curve. But some spikes of large amplitudes are seen inbetween. These may be due to the interpolation which is carried out while decomposing as well reconstructing the signal. Otherwise the curve is smooth (Fig. 3.14).

Fig 3.10 EXPONENTIAL WITH SPIKES

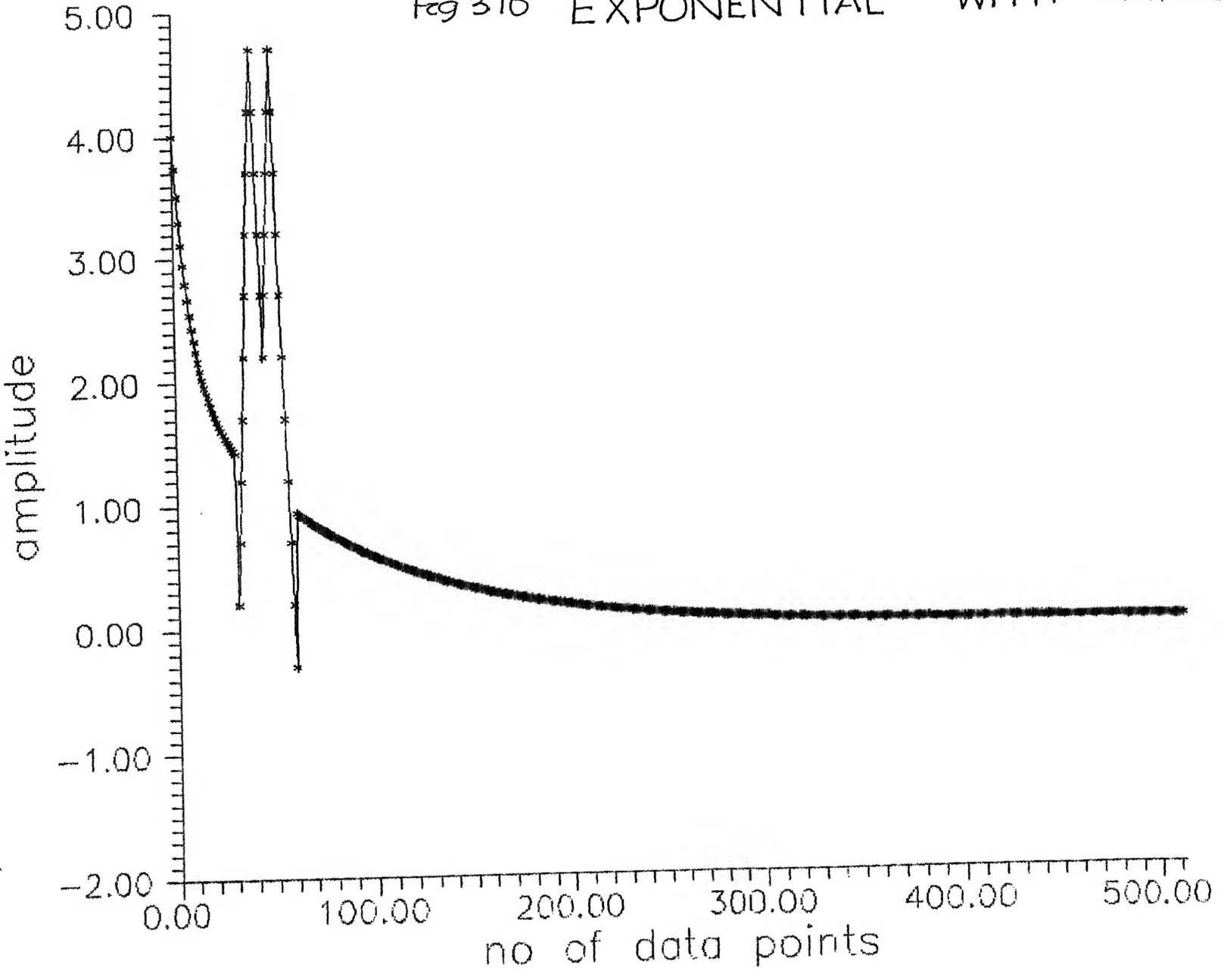

Fig 3.11 reconst. of exponential with spikes (cubic spline)

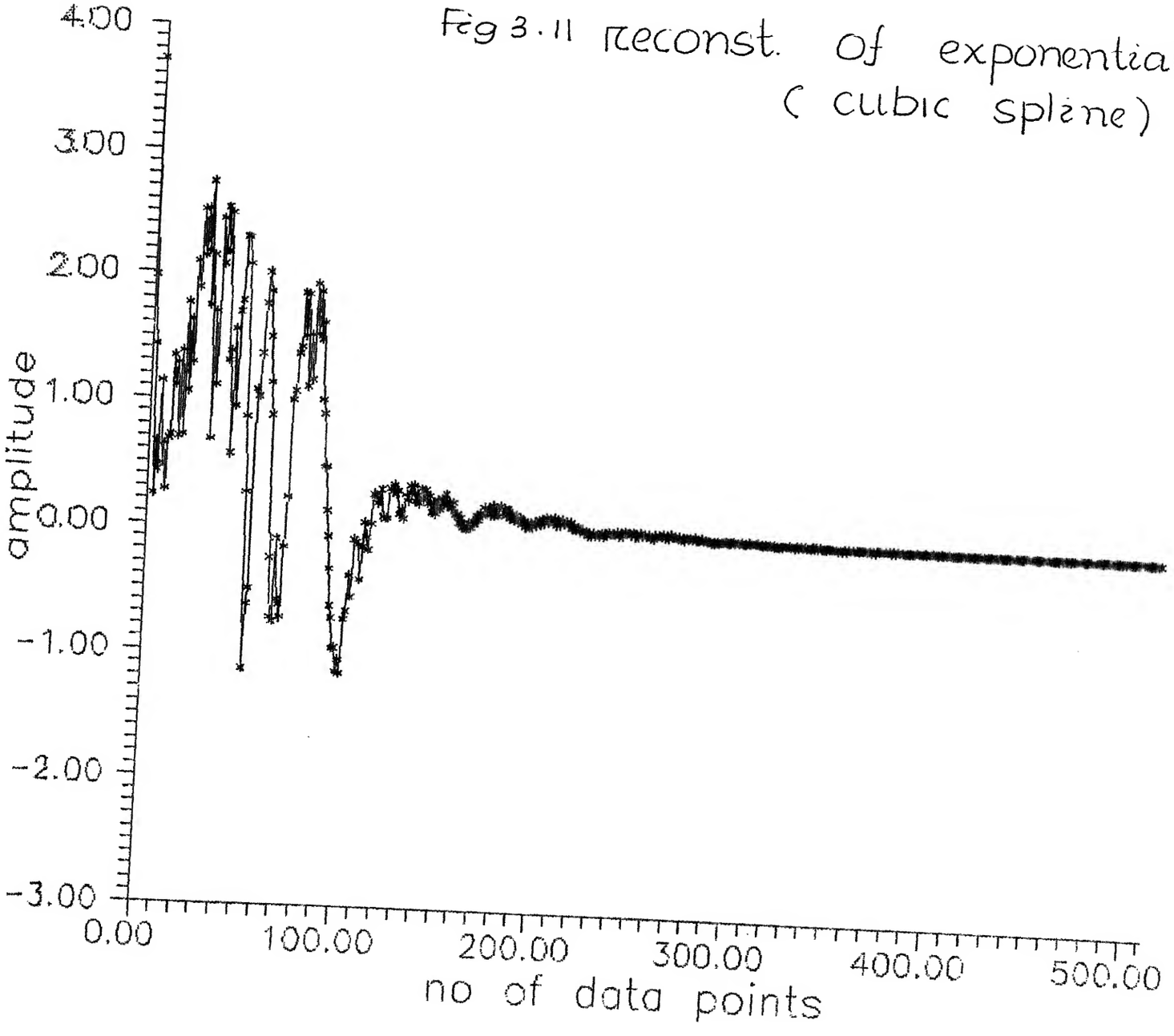

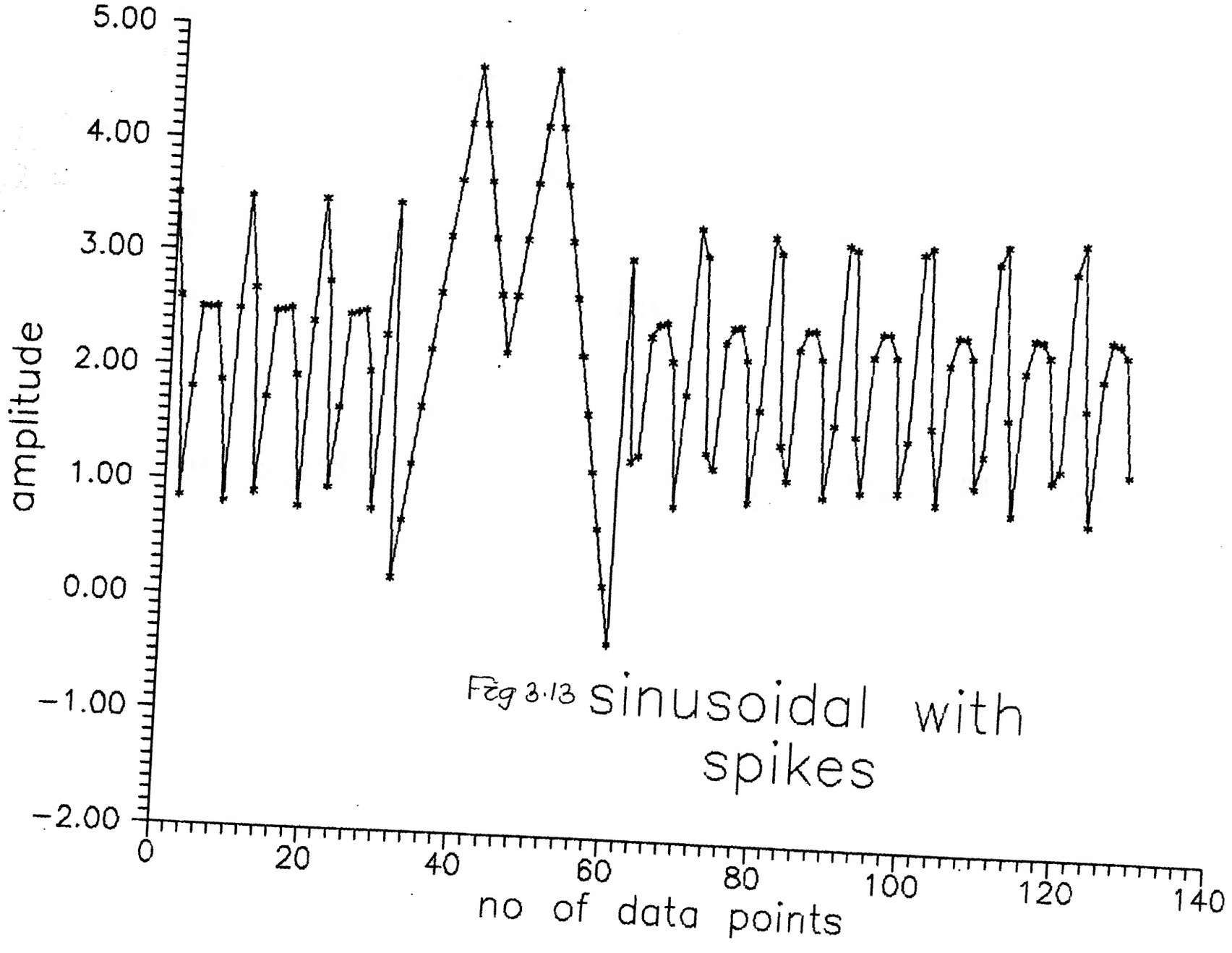

Fig 3.13 sinusoidal with spikes

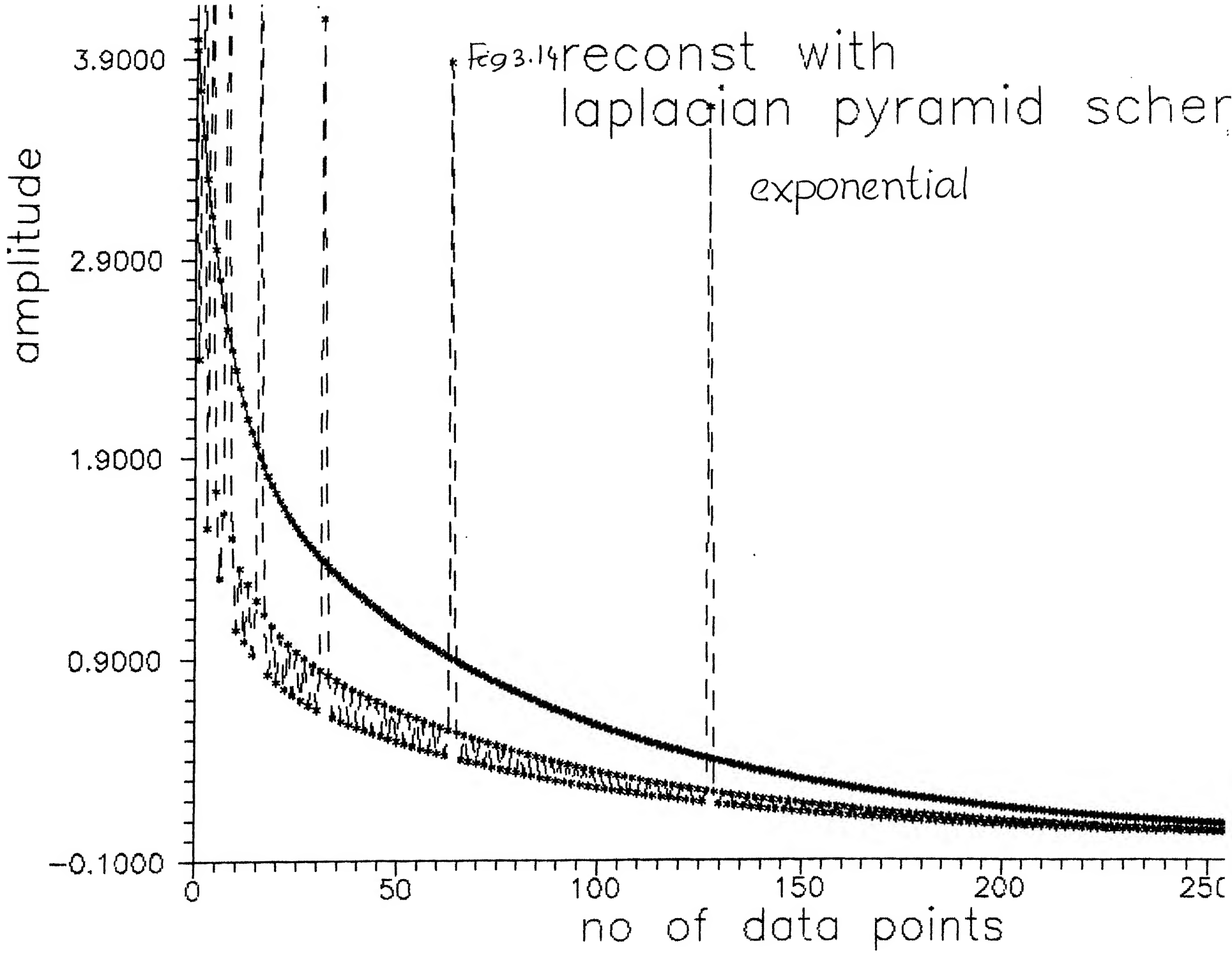
Fig 3.14 reconst with
laplacian pyramid scher
exponential
amplitude
3.9000
2.9000
1.9000
0.9000
-0.1000
0
50
100
150
200
250
no of data points

(ii) Sinusoidal :

This curve by undergoing decomposition and reconstruction through Laplacian Pyramid scheme, does follow the original curve. But again some spikes are visible in the reconstructed waveform. These may be due to the reasons as stated above for exponential curve (Fig. 3.15).

3.6 ENERGY PLOTS OF DETAIL SIGNAL

The energy of the detail signal for the sinusoid with spikes at various resolutions such as 0.5, 0.25, 0.125, and 0.0625 was found out and were plotted to observed that there were two distinct spikes occurring in all cases (Figs. 3.16. 3.17, 3.18 and 3.19).

3.7 SEPARATION OF EXPONENTIALS [5]

The separation of exponentials is an age old problem. The idea is to find out the number of exponentials which make a set of data points. Also it is required to estimate the amplitude and time constant of the same exponentials. This problem has been dealt with at various stages. One of them is modelling approach. In this thesis, this problem has been taken up for tackling from the wavelet transformation point of view. The basic motivation for looking into the problem in this context is that when we carry out wavelet transform, the transformed data carry more information compared to the original data.

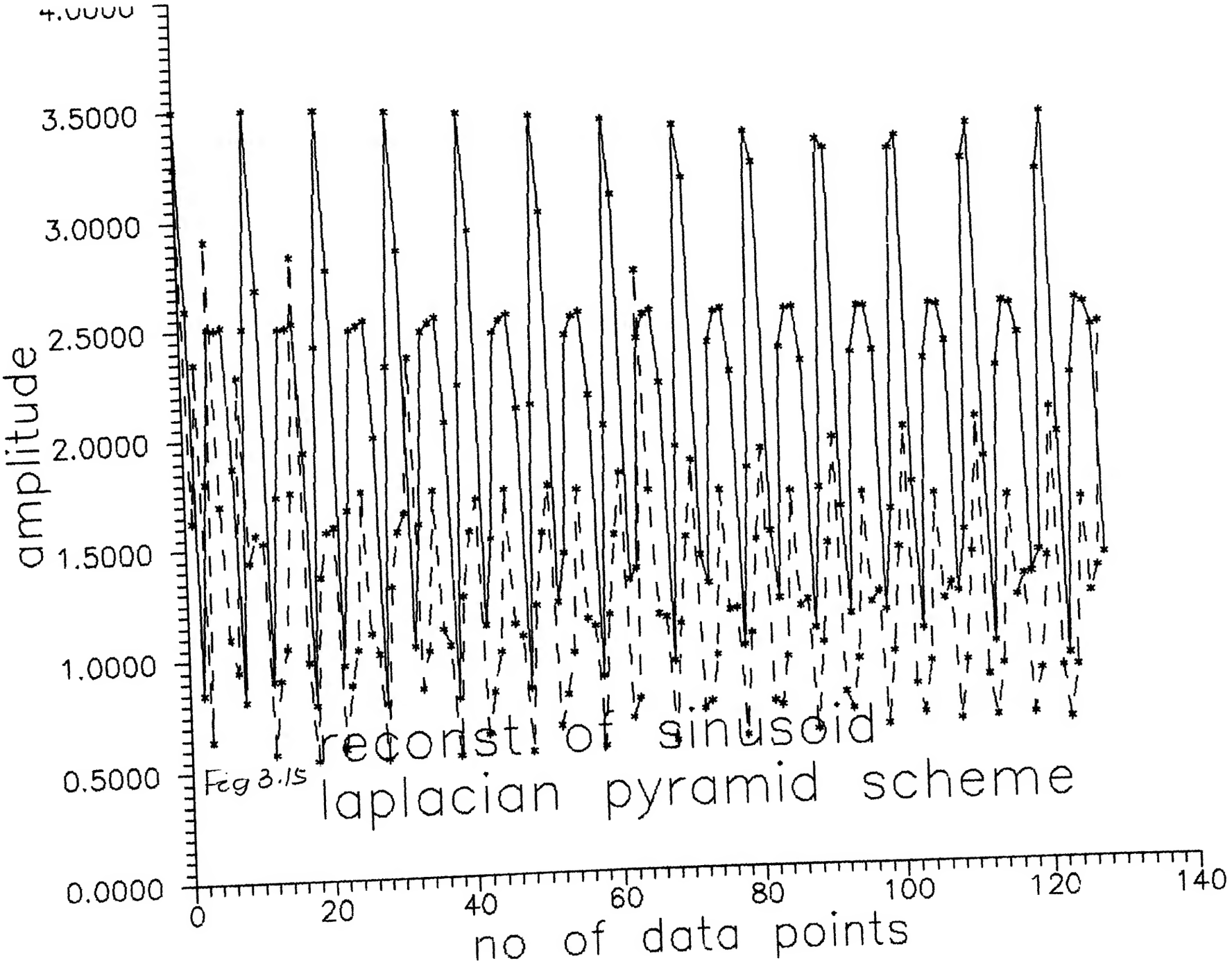
4.0000
3.5000
3.0000
2.5000
2.0000
1.5000
1.0000
0.5000
0.0000
amplitude
0
20
40
60
80
100
120
140
no of data points
recons! of sinusoid
laplacian pyramid scheme

Fig 3.15

Fig 3.16

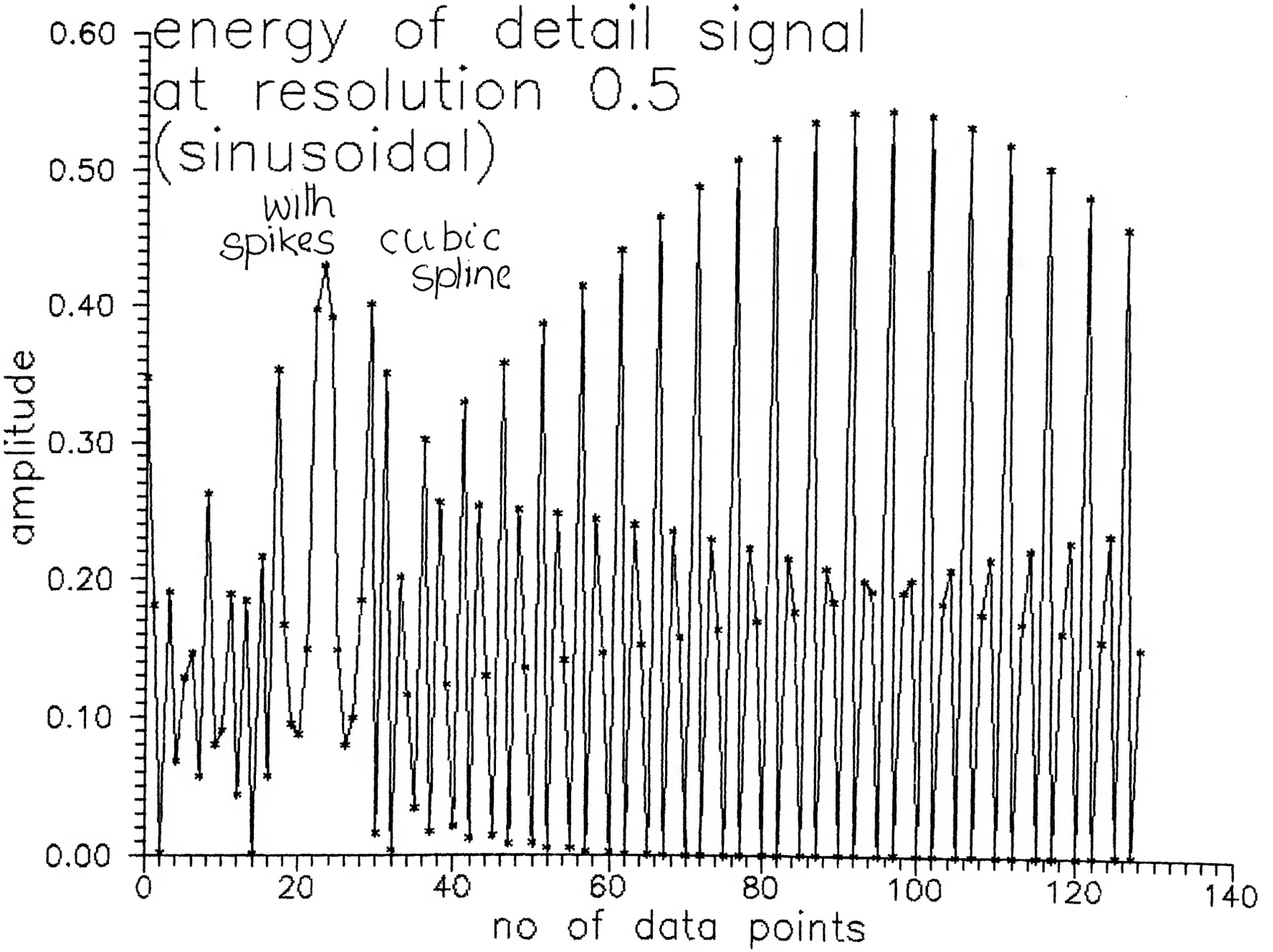
energy of detail signal
at resolution 0.5
(sinusoidal)
with spikes
cubic spline
amplitude
0.60
0.50
0.40
0.30
0.20
0.10
0.00
0
20
40
60
80
100
120
140
no of data points

Fig 3.17

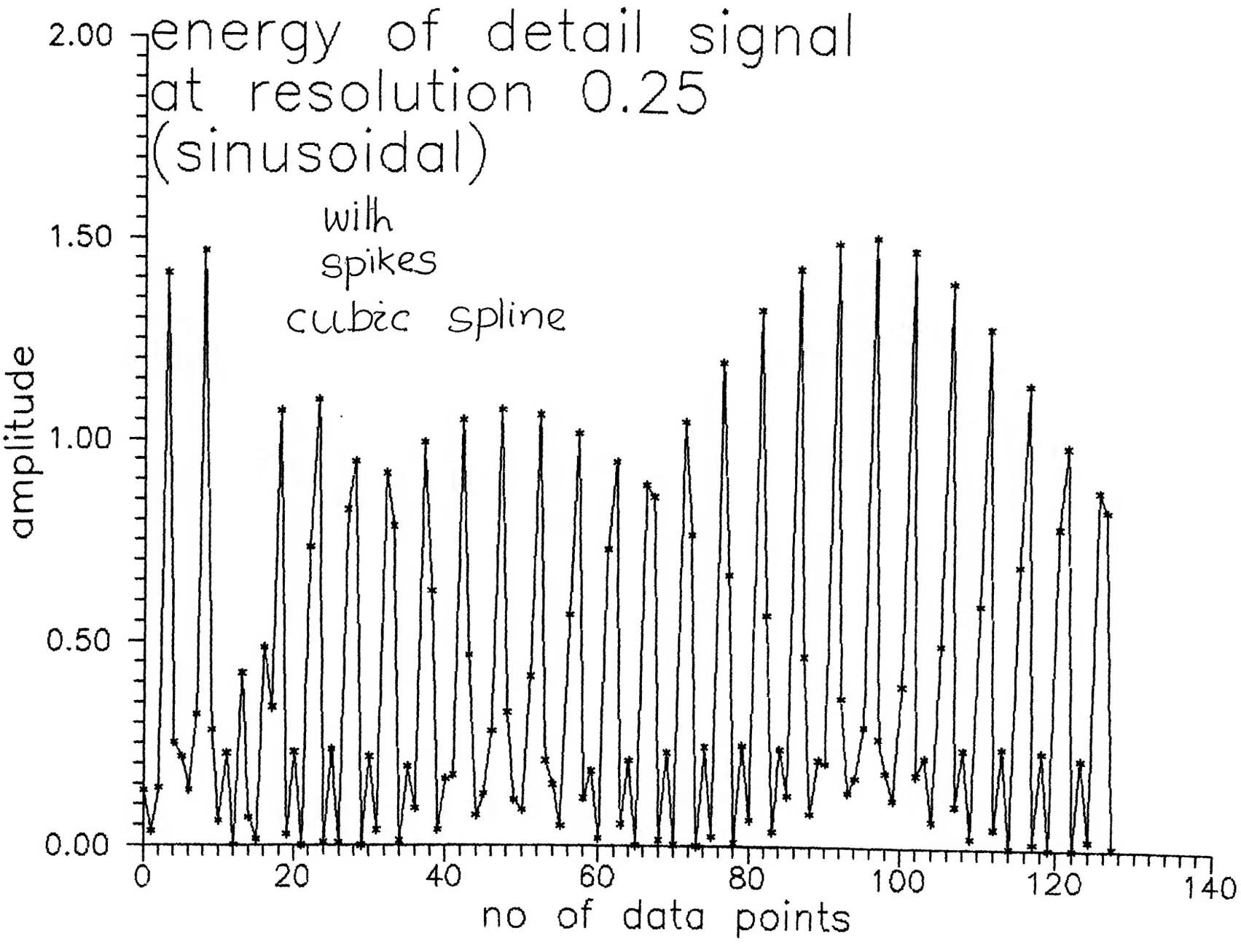
energy of detail signal
at resolution 0.25
(sinusoidal)
with
spikes
cubic spline
amplitude
2.00
1.50
1.00
0.50
0.00
0
20
40
60
80
100
120
140
no of data points

Fig 3.18

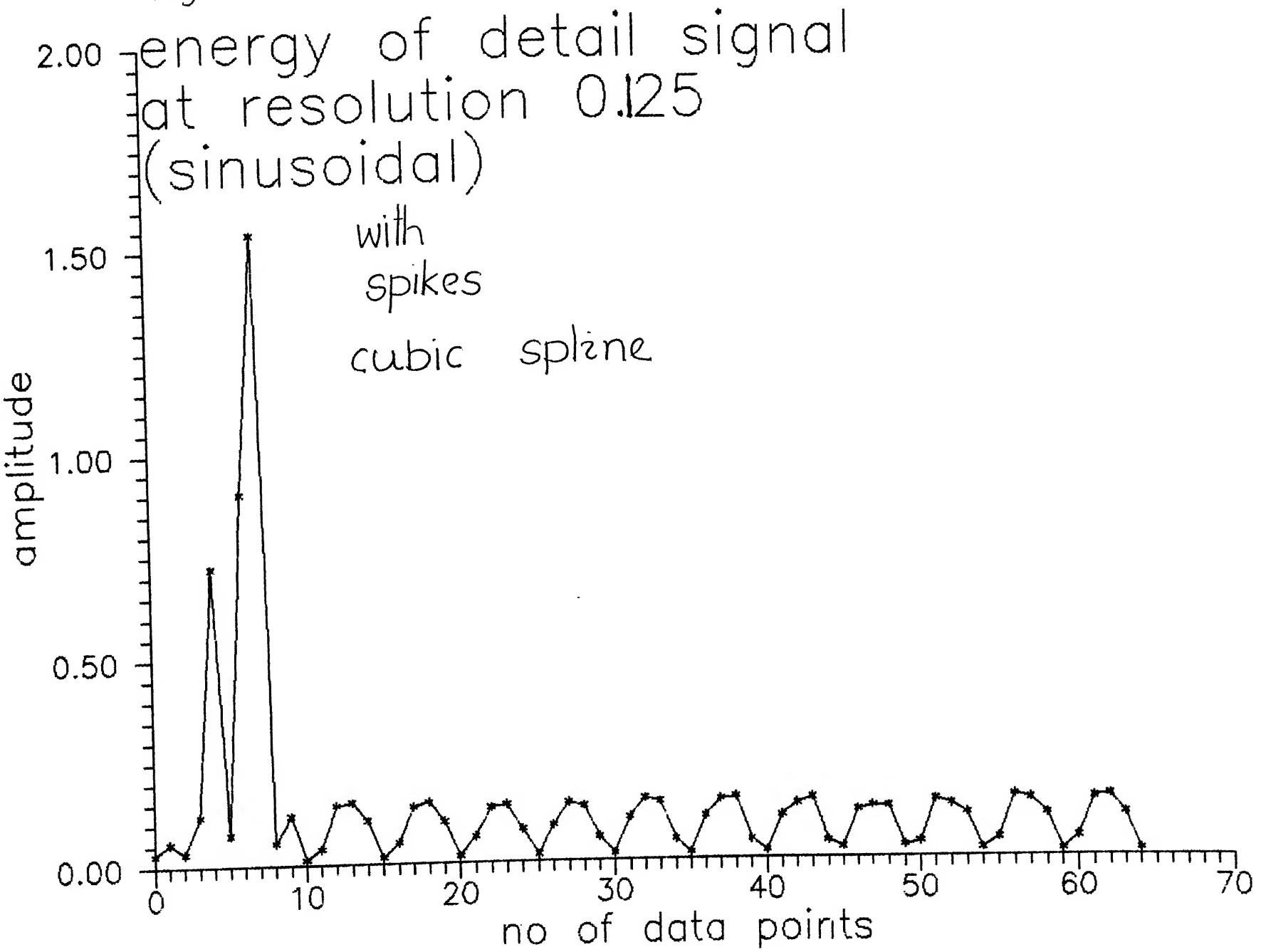
energy of detail signal
at resolution 0.125
(sinusoidal)
with
spikes
cubic spline
2.00
1.50
1.00
0.50
0.00
amplitude
0
10
20
30
40
50
60
70
no of data points

Fig 3.19

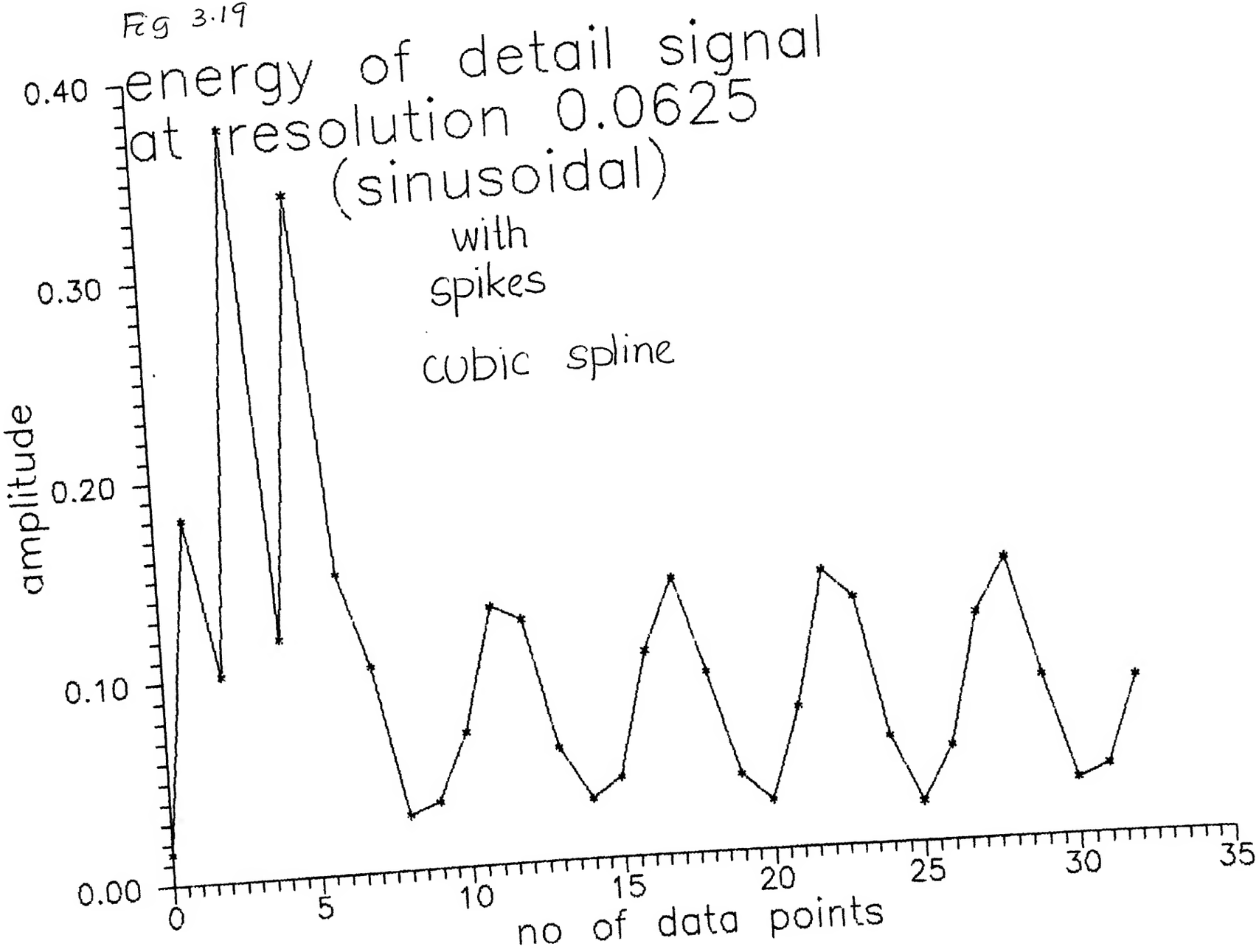
energy of detail signal
at resolution 0.0625
(sinusoidal)
with
spikes
cubic spline
amplitude
0.40
0.30
0.20
0.10
0.00
0
5
10
15
20
25
30
35
no of data points

When we examine the decomposition and reconstruction of the exponential signal with the help of linear spline function we find that there is a dip at the beginning of the reconstructed signal before it converges to zero. That dip may be intepreted as an exponential with large time constant. We reconstructed the exponential with large time constant taking linear spline into account. Then we kept adding to it another exponential by varying its amplitude and time constant and these curves were decomposed and reconstructed. Now these were matched with the reconstructed curve of the original exponential function. Then we tried to find out which is the one closest to the original curve.

The original exponential curve was

$$f(x) = 2 \exp\left[-0.01\ x\right] + 2 \exp\left[-0.1\ x\right]$$

The exponential which was kept fixed was 2exp(-0.01 x). The exponential which was varied was 2exp(-0.1 x). It was varied in the following manner :

(i) Amplitude constant and time constant varying :

The amplitude was kept constant at 2, but the time constant were varied as 0.025, 0.05 and 0.09 respectively (Figs. 3.20 and 3.21).

(ii) Amplitude varying and constant time constant :

In this case the time constant was kept at 0.1, but the amplitude of the exponential was varied as 0.5, 1 and 1.5 respectively (Figs. 3.22 and 3.23).

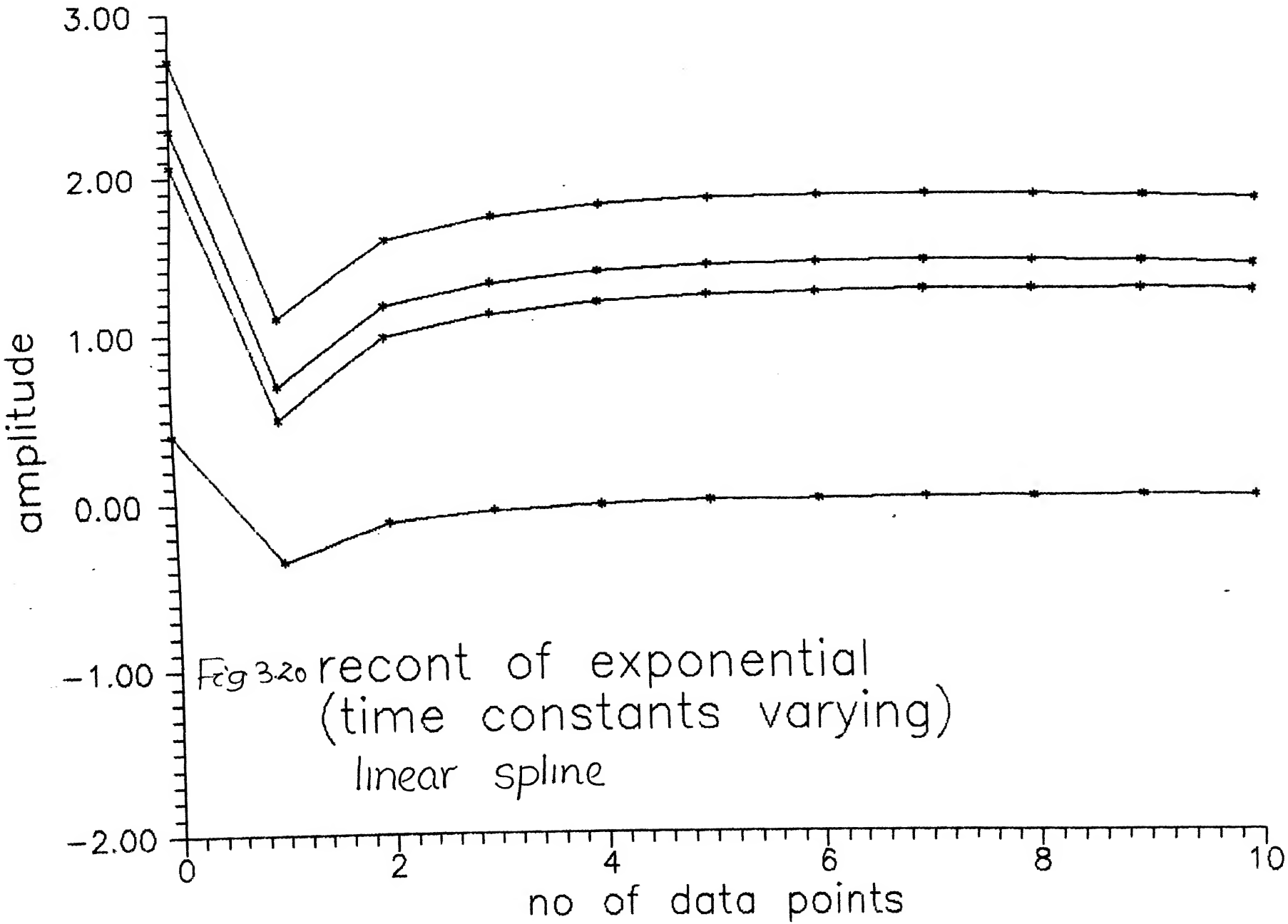

Fig 3.20 recont of exponential
(time constants varying)
linear spline

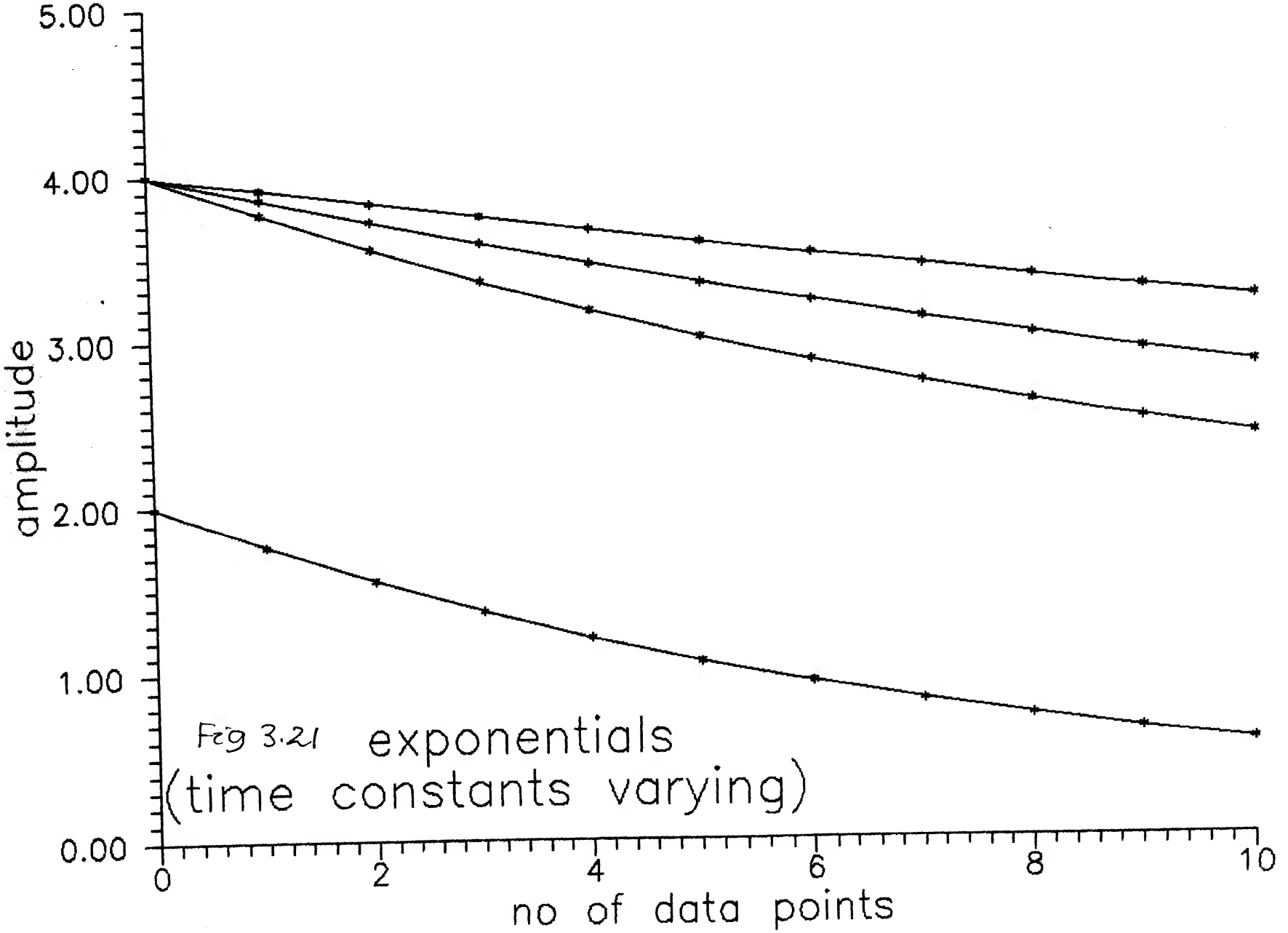

Fig 3.21 exponentials (time constants varying)

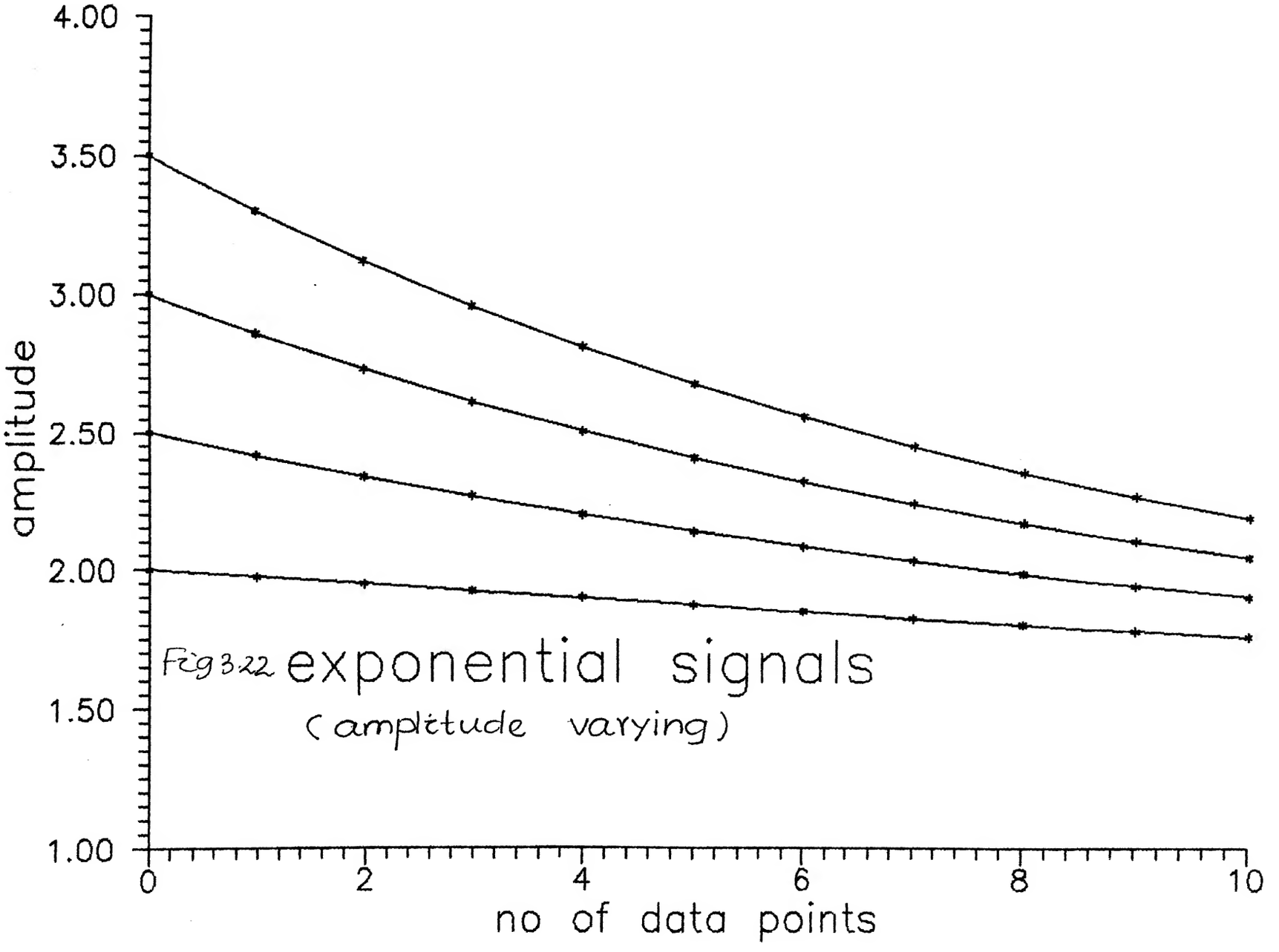

Fig 3.22 exponential signals
(amplitude varying)

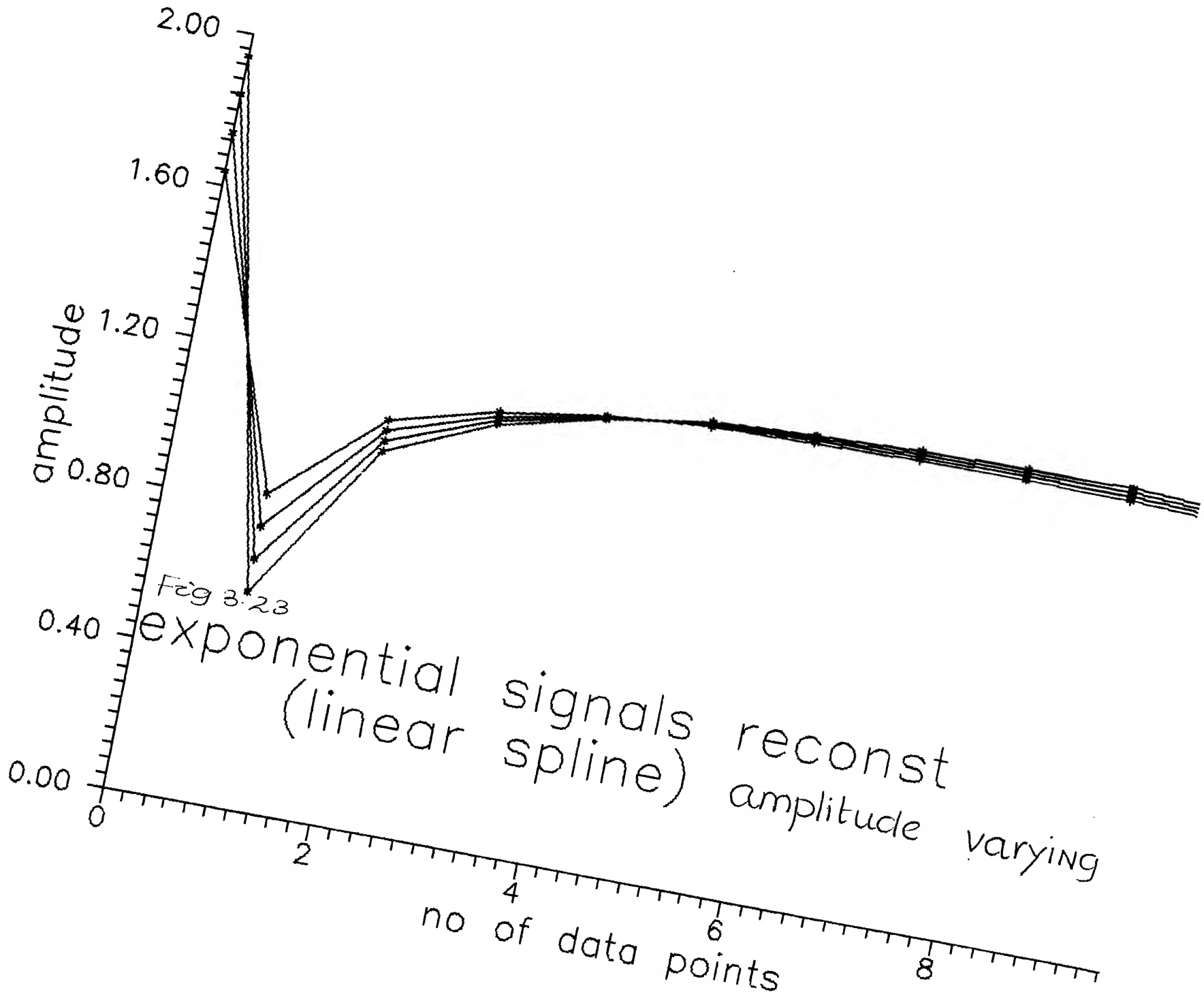
2.00
1.60
1.20
0.80
0.40
0.00
amplitude
0
2
4
6
8
no of data points
exponential signals reconst
(linear spline) amplitude varying

Fig 3.23

It was observed that in the first case, the reconstructed exponential varied from each other and also from the original one. The exponential with time constant 0.09 was the closest to the original. But in the other case, when the amplitude is varied it was found out that all of them follow each other very closely and are very closed to original curve.

CHAPTER - 4

CONCLUSIONS

In this paper, we reviewed the application of wavelet decomposition and reconstruction of signals from several viewpoints. We covered exponential and sinusoidal signals showing that such a decomposition and reconstruction can be applied to such signals. We described the mathematical properties of these decomposition. We first analysed different types of orthogonal basis functions and the corresponding wavelets. The properties of a window Fourier transform have been reviewed and a comparison has been drawn between the transform and the wavelet transform.

We described the classical pyramidal multiresolution algorithms and the wavelet approach to multiresolution decompositions. The difference of information between approximation of a function at two different resolutions is computed by decomposing the function into a wavelet orthonormal basis. We also explained the relationship between the orthonormal wavelet and quadrature mirror filter. The application of the wavelet decomposition and reconstruction to signals such as exponential and sinusoidal was carried out. It was found out that the linear spline is more applicable to exponential signals where there is a smooth reconstruction and also elimination of noise.

As far as the separation of exponentials is concerned the problem was tackled from the wavelet point of view. It was found that while doing decomposition and reconstruction with linear

spline one of the exponentials which constitutes the original data is exposed. The other one is found out by trial and error method. This problem may be tackled by fitting a polynomial curve of exponentials to the reconstructed data.

LIST OF REFERENCES

[1] Stephane G. Mallat, "Multifrequency Channel Decompositions of Images and Wavelet Models", IEEE Trans. Accoust., Speech, Signal Processing, Vol. ASSP-37, pp. 2091-2110, Dec. 1989.

[2] Stephane G. Mallat, "A Theory for Multiresolution Signal Decomposition : The Wavelet Representation", IEEE Trans. Pattern Analysis and Machine Intelligence, Vol. II, pp. 674-693, July 1989.

[3] I. Daubechies, "Orthonormal bases of compactly supported wavelets", Commun. Pure Appl. Math., Vol. 41, pp. 909-996, Nov. 1988.

[4] Olivier Rioul and M. Vetterli, "Wavelets and Signal Processing", IEEE SP Magazine, Oct. 1991.

[5] C. Lanczos,, "Applied Analysis", Prentice-Hall Inc., May 1961. Chapter 4